

## Temperature-triggered *in situ* forming lipid mesophase gel for local treatment of ulcerative colitis

Marianna Carone<sup>1§</sup>, Marianne R. Spalinger<sup>2§</sup>, Robert A. Gaultney<sup>3§</sup>, Raffaele Mezzenga<sup>4</sup>, Aart Mookhoek<sup>3</sup>, Philippe Krebs<sup>3\*</sup>, Gerhard Rogler<sup>2\*</sup>, Paola Luciani<sup>1\*</sup>, Simone Aleandri<sup>1\*</sup>

§Contributed equally; \*Contributed equally

<sup>1</sup> Department of Chemistry, Biochemistry and Pharmaceutical Sciences, University of Bern, Bern, Switzerland

<sup>2</sup> Department of Gastroenterology and Hepatology, University Hospital Zurich, University of Zurich, Zurich, Switzerland

<sup>3</sup> Institute of Pathology, University of Bern, Bern, Switzerland

<sup>4</sup> Laboratory of Food & Soft Materials, Institute of Food, Nutrition and Health, IFNH; Department for Health Sciences and Technology, D-HEST, ETH Zurich, Switzerland

\*Correspondence to be sent to: E-mail: [philippe.krebs@unibe.ch](mailto:philippe.krebs@unibe.ch); [gerhard.rogler@usz.ch](mailto:gerhard.rogler@usz.ch); [paola.luciani@unibe.ch](mailto:paola.luciani@unibe.ch); [simone.aleandri@unibe.ch](mailto:simone.aleandri@unibe.ch)

### Abstract

Ulcerative colitis (UC) is a chronic inflammatory bowel disease affecting the colonic mucosa. There is no cure for UC and its chronic relapsing/remitting nature strongly affects patient quality of life. Current treatment options frequently have significant side effects and remission rates are limited raising a demand for new treatment strategies. Novel therapeutic approaches that could maximize the drug concentration at the site of inflammation with minimal systemic exposure, like topical applications, would address this unmet clinical need. To date, few drug delivery systems (DDSs) have been designed to topically convey small molecules to the rectum and left-sided colon. Here, we developed and tested a drug delivery platform for topical treatment of UC based on a temperature-triggered *in situ* forming adhesive lipid gel (TIF-Gel). Due to its soft, gel-like consistency, its high encapsulation efficacy, and its drug-controlled release, TIF-Gel suggests a more patient-friendly and effective application with respect to the rectal formulations currently available.

Capitalizing on the biocompatible and biodegradable self-assembled structure of lipid mesophases (LMPs), we loaded TIF-Gel with tofacitinib (TOFA; a hydrophilic inhibitor of the enzymes Janus kinase 1 and 3) or TAC (a hydrophobic immunosuppressive drug), both of which are indicated in the treatment of UC. We designed and fully characterized our biocompatible lipid formulation *in vitro* and tested it *in vivo* using two different murine models of inflammatory bowel disease: chemically-induced and T cell transfer-mediated. Both approaches (TIF-Gel-TOFA and TIF-Gel-TAC) led to reductions in colitis disease severity and intestinal inflammation compared to vehicles, therefore showing therapeutic efficacy.

Overall, our findings show that TIF-Gel can deliver drugs locally to the colonic mucosa to mitigate intestinal inflammatory disease in a pre-clinical model. They also suggest that, in a clinical setting, TIF-Gel might provide a patient-friendly approach to improve colitis while allowing for a reduction of the adverse effects associated with a systemic therapy.

## Introduction

Ulcerative colitis (UC) is a chronic remitting-relapsing inflammatory disorder of the large intestine, involving the colonic and rectal mucosa (1). Clinically, 75% of patients suffer from left sided colitis or proctitis but the inflammation can spread upward in a continuous manner and involves the colon partially or entirely (2). There is no known cure for UC and the chronic relapse and remission often result in patient disability (1, 2). All treatments currently recommended by the European Crohn's and Colitis Organization (ECCO) and American Gastroenterological Association (AGA) struggle to deliver the desired remission rates, and many patients must cycle through several different therapies to achieve remission (3, 4). Following a step-up approach, the first line treatment of mild to moderate left-sided UC or pancolitis is 5-aminosalicylic acid (5-ASA, combined topical and oral administration) for the induction of remission. For refractory patients and in severe disease cases, systemic corticosteroids, azathioprine, 6-mercaptopurine, monoclonal antibodies (such as infliximab, an anti TNF- $\alpha$ ; vedolizumab, an anti  $\alpha$  $\beta$  integrin; and ustekinumab, IL-12/IL-23 blockade) and ozanimod (a sphingosine 1-phosphate receptor modulator) are the treatments of choice to obtain remission (4–8). Biological-based therapies may have considerable side effects including systemic toxicity, resulting in recurrence of opportunistic infections, psoriasis, a lupus-like syndrome, and loss of response to therapy over time (9–13).

Recently, tofacitinib (TOFA), a small-molecule inhibitor of the enzymes Janus kinase 1 and 3 (JAK3 and JAK1, respectively) (14), was approved by European and US regulators for the oral treatment of UC in patients who had intolerance or a loss of response to biologic drugs. Its oral administration is preferred by many patients as compared to biologics in maintenance of remission and endoscopic improvement (15, 16). In steroid-refractory UC, the use of tacrolimus (TAC) – a macrolide that inhibits T-lymphocyte activation – is recommended (17). However, TOFA and TAC showed dose-dependent adverse effects when administered systemically (e.g. nephrotoxicity, thromboembolic complications, headache, metabolic disorders) in a significant fraction of patients (18–21), which may require discontinuation of the treatment in some cases and limits the dosages that can be administered (21). Taken together, the side effects of these systemically administered drugs must be weighed in patient management against the potential benefits of UC treatment. If not for the limiting side effects, higher drug concentrations would likely have a higher efficacy.

The specific localization of the disease to the colon encourages the use of topical therapies (22). Indeed, delivery via the rectal route is a safe therapeutic approach that can maximise the drug concentration directly at the site of inflammation while minimizing systemic exposure. 5-aminosalicylic acid (5-ASA) or budesonide in rectal preparations as enema or foam are routinely used as first-line treatment for UC (23, 24). The rectal administration of 5-ASA in UC patients has been shown to be significantly more efficient than oral administration (25–30). The efficacy of rectal administration is further supported by the finding that steroid-refractory ulcerative proctitis has been managed by topically administered TAC as ointment (27, 31), suppository (32) or enema (20, 21, 30).

Although clinical studies have shown that rectal 5-ASA preparations are more effective than oral preparations, these treatments are still rarely prescribed (33). The efficacy of conventional enema-based formulations is intrinsically limited by their insufficient retention in the colon (34) and faecal urgency associated with the large volumes administered (35). The required retention time – at least 20 minutes – together with frequent dosing negatively affect patient compliance (36).

To address these drawbacks, and to improve either the performance of the topical formulation or the therapeutic outcome of the delivered drug, we propose, herein, a gel platform that employs rectal temperature as a trigger for the formation of a highly viscous adhesive depot system (TIF-Gel). TIF-Gel is a lipidic mesophase (LMP) based formulation, a versatile delivery system able to protect and release the incorporated drugs slowly *in vivo* (37, 38). Upon hydration, monoacylglycerol lipids such as monolinolein (MLO, generally recognized as safe for human and/or animal use by the FDA) can self-assemble in different arrangements. By increasing the water content, the less viscous lamellar (*L*) phase transforms first to an *Ia3d* and then to a *Pn3m* cubic phase (*Q*) which are similar in appearance and rheology to a high viscous cross-linked hydrogel (39). To overcome the hurdle of administering a highly viscous gel, not only water (40) but also temperature can be used as a trigger to tune the viscosity of the system. Increasing the system's temperature, indeed, induces a transition from the *L* phase to a *Q* phase (with *Ia3d* symmetry) (39, 41).

Considering the peculiarity of the rectal milieu, characterized by a low volume and with a composition highly affected by age, biological sex and pathology (42), water is not the most suitable trigger for an *in situ* gelation. Thus, rectal temperature is the ideal condition to activate the transformation of the precursor *L* phase into the cubic phase gel. The TIF-Gel was then loaded with the hydrophilic TOFA or hydrophobic TAC and the therapeutic suitability of the drug-loaded TIF-Gel was tested and validated *in vivo* in the contexts of chemically and T cell transfer induced colitis in mice—two established models of inflammatory bowel disease (IBD) (43, 44). Results demonstrate that our TIF-Gel provides a valuable approach to effectively administer these drugs locally to the inflamed colonic mucosa resulting in sustained drug release. Furthermore, our findings suggest that the TIF-Gel enhances the localized activity of these anti-inflammatory drugs while potentially reducing the risk of side effects. Thanks to the higher viscosity that the gel develops in the rectal environment, we observed a low leakage of the gel after administration in mice.

Overall, we expect that our TIF-Gel may translate to a topical mucosal therapy with high patient friendliness, by concomitantly decreasing problems with retention, bloating, and urgency, and therefore increasing therapy compliance.

## RESULTS

### Physico-chemical characterization of TAC- and TOFA-loaded TIF-Gel

To decrease the drugs' adverse effects and to improve either the performance of the topical formulation or the therapeutic outcome of the delivered drug, we designed and developed a gel formulation based on the concept that at 25 °C and in the presence of a low percentage of water, MLO forms a lamellar (*L*) phase with a lower structural strength with respect to the cubic phase (*Q*), resulting in a formulation easier to administer and able to treat remote tissue areas, as depicted in **Figure 1a**. Once applied into the rectum, the precursor *L* phase gradually absorbs heat (and the available amount of water) from the body and rapidly converts into the cubic phase, contributing to the formation of a depot *in situ*. The gel, therefore, allows local release of the incorporated drug in a sustained fashion.

In a first step, we used small angle X-ray scattering (SAXS) measurements to determine the optimal amount of water needed to obtain a lamellar phase which provides a transition to the cubic phase at 38 °C. (**Figures 1b** and **1c**). The X-ray beam directed at the gel results in a scattering pattern with a set of maxima, that correspond to sharp Bragg

reflections characteristic of the long-range positional order. The sequence of Bragg reflections (and their ratio; listed in **Figure 1a**) identifies the symmetry of the mesophase studied (45).

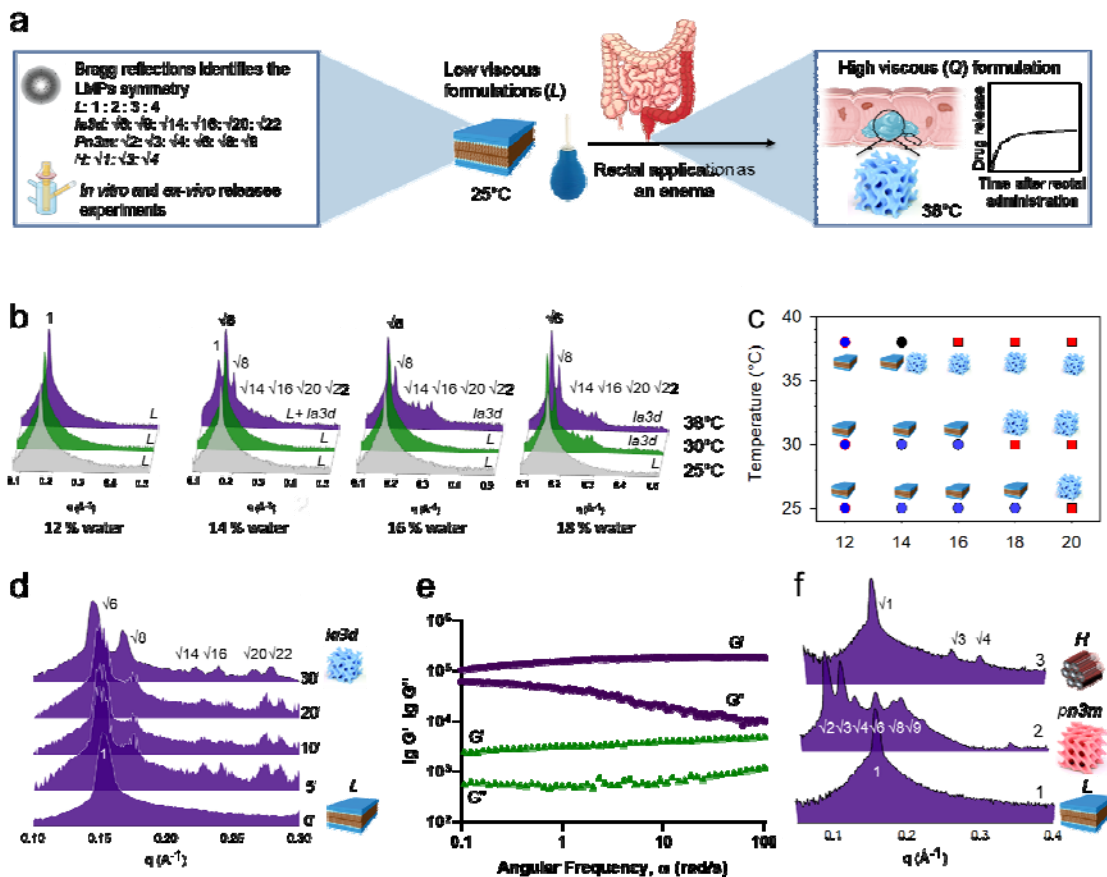


**Figure 1.** *In vitro* characterizations of the TIF-Gel: a) schematic depiction of the *in vitro* characterization and the mechanism of the gel formation. b) SAXS spectra acquired at different temperatures (25, 30 and 38  $^{\circ}\text{C}$ ; bottom, middle and top spectra, respectively) on gels containing increasing amount of water (12%, 14%, 16% and 18 % w/w) and (c) the obtained partial phase diagram (blue circles: *L*; black circles: coexistence of *Ia3d* + *L*; red squares: *Ia3d*). (d) SAXS spectra acquired at different times (5, 10, 20 and 30 min) after incubation at 38  $^{\circ}\text{C}$ ; (e) frequency sweep at the end of the release experiments (blue symbols) and at the beginning of the experiment (green symbols); (f) SAXS before (1) and after incubation of LMPs in HEPES buffer (2) and in HEPES buffer enriched with 1000 U/mL of lipase (3). The LMPs cartoons (*L*; cubic *ia3d*, cubic *pn3m* and hexagonal) are adapted for Alendri *et. al.* (38).

As shown in **Figures 1b** and **1c**, with 12% water the Bragg reflections characteristic of *L* phase were present at 25 and 38  $^{\circ}\text{C}$ . Hydrating the MLO to 14% water led to a lamellar structure at 25  $^{\circ}\text{C}$  and a coexistence of *L* and *Q* structures (with an *Ia3d* geometry) at 38 $^{\circ}$ , whereas increasing the amount of water up to 18% w/w induced the *L*  $\rightarrow$  *Q* transition already at 30  $^{\circ}\text{C}$ . On the other hand, a mesophase composed by 16% w/w of water and 84% w/w of MLO gives Bragg reflections characteristic of the lamellar structure at 25  $^{\circ}\text{C}$  and a transition to a *Q* structure (with a *Ia3d* geometry) at 38 $^{\circ}$ , i.e. the rectal temperature.

The reflections characteristic of this *L* phase (containing 16 % water) adopt those characteristic of a *Q* phase after only 5 min of incubation at 38 °C (**Figure 1d**), indicating a rapid conversion of the lamellar precursor into the *Ia3d* cubic structure (39), making it particularly suited for rectal administration. The diverse topologies of the mesophases were confirmed by the different viscoelastic regimes identified by rheological (frequency sweep) measurements. Specifically, the precursor *L* phase had a low structural strength, as indicated by the lower value of storage modulus and loss modulus ( $G'$  and  $G''$ , respectively) with respect to the viscoelastic *Q* phase. This resulted in a less viscous pseudoplastic gel characterized by extensive energy dissipation mechanisms associated with the parallel slip of the lamellae. In simulated administration conditions, increasing the temperature and water availability resulted in swelling of the structure corresponding to a *Q* phase transition (where both  $G'$  and  $G''$  are higher than those obtained for *L* phase; **Figure 1e**).

To prove the occurrence of the expected transition, a series of SAXS experiments were carried out after the gel was soaked in 1 mL of HEPES (or, alternatively, in a buffer solution containing lipase) and incubated at 38 °C for 8 h. As shown in **Figure 1f**, the *L* phase absorbed heat and water during the release experiments reaching a cubic (*pn3m*) phase with a lattice parameters ( $a = 8.7$  nm) and a water channel ( $d_w = 4$  nm) comparable with those obtained for a *Pn3m* phase at its maximum hydration level (46). The presence of lipase (1000 U/mL) hydrolysed the ester group of MLO inducing a transition from *Q* → Hexagonal phase (*H*) (47), with the latter not linked to a burst release phenomenon (**Figure 2**). Based on this initial characterisation, we chose an 84% MLO and 16% water formulation for subsequent *in vitro* and *in vivo* studies, which had suitable rheological properties to pass through a small diameter animal feeding needle (size 20G) to further expand into a sponge-like system once injected into the rectum.

### **Drugs are efficiently encapsulated and released from TIF-Gel**

In order to properly use TIF-gel as a treatment option, the initial and phase change characteristics must remain constant even after it has been loaded with the desired compounds. To evaluate the influence of the guest drugs on the phase identity, TOFA (a hydrophilic inhibitor of the JAK 1 and 3) and TAC (a hydrophobic immunosuppressive drug) loaded-mesophases were independently prepared and analyzed with SAXS. Notably, the entrapment of drugs (5 mg of TOFA or 1 mg of TAC in 100 mg of gel – 5 or 1% w/w, respectively) (**Figures 2a** and **2d**) did not affect the phase identity and thermal behaviour of the carrier gel and the rectal temperature still induced a transition from *L* → *Q* phase. When hydrated with water, the lipid/drug mixtures form the lamellar structure and the totality of the drugs are embedded in the gel with a 100% encapsulation efficacy.

In the *in vitro* release experiments, drug-loaded TIF-Gel formulations were placed in the donor chamber of a vertical Franz cell (a commonly used apparatus to assess the drug release from a semisolid dosage formulation in preclinical studies; depicted in **Figure 2**) and kept separated from the acceptor chamber by a polycarbonate membrane with pore diameter of 3  $\mu\text{m}$ , which allows the passage of the free drugs only (48).

Contrary to the small intestine, for which different *in vitro* models are established (49–51), for colon tissues only animal models are available and are mostly used in pre-clinical studies (52, 53). To bypass this limitation, an *ex vivo* approach was employed in which tissues isolated from healthy rat colon were used as natural membrane replacing the polycarbonate membrane detailed above (54). The 3D gel network retains the TOFA (hydrophilic drug) and slowly releases it in both the *in vitro* and an *ex vivo* setups (**Figures 2b** and **2c**, respectively). The same sets of

experiments were also carried out for the TAC-loaded gel. Results for this hydrophobic drug mirrored those of the hydrophilic TOFA in both *in vivo* and *ex vivo* experiments, reflecting the flexibility of this vehicle (**Figure 2e,f**).

Notably, the presence of lipase in our experimental conditions did not induce disassembly of the gel with consequent burst release of the drug, as reported for another lipid-based gel, developed to topically treat UC (55). In this study, addition of the enzyme (*Thermomyces lanuginosus* lipase) induced a responsive release (+20% of drug released) from the hydrogel only after 24 h. In comparison, TAC and TOFA were released from our TIF-Gel within only 8 h, a time span more compatible with the retention time of rectally administered dosage forms. Interestingly, the presence of 10 mg of the drugs (10% w/w of both TOFA and TAC) did not affect the phase identity and the transition temperature of the gel, which gives a lamellar phase at room temperature and a cubic (*Ia3d*) phase at 38 °C (see SI; **Figure S1**), as wished. This demonstrates that the administration of a low volume of TIF-Gel could indeed deliver high amount of drug, prospectively reducing the urgency associated with the application of a large volume (56).

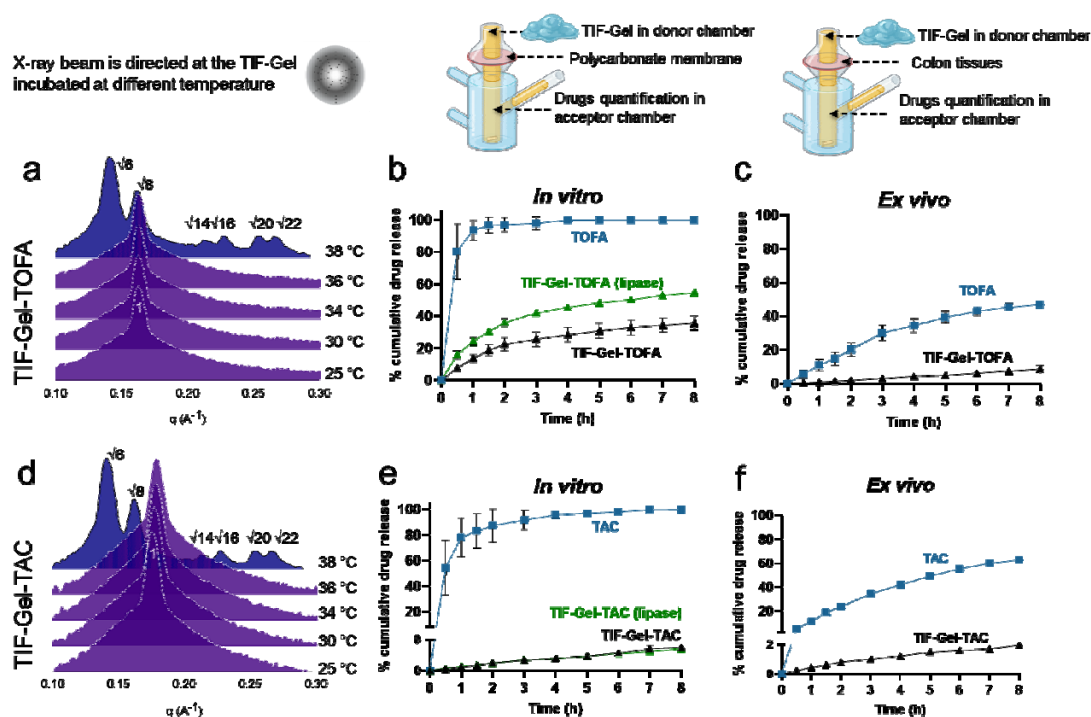


**Figure 2.** *In vitro* and *ex vivo* characterizations of the drug loaded TIF-Gel: (a) TOFA-loaded gel (TIF-Gel-TOFA) SAXS spectra acquired at different temperatures; (b) *in vitro* release of free drug (TOFA, blue line) and TIF-Gel-TOFA in HEPES buffer (black line) and in the presence of lipase (green line); (c) *ex vivo* release of free drug (TOFA, blue line) and TIF-Gel-TOFA (black line); (d) TAC loaded LMPs (TIF-Gel-TAC) SAXS spectra acquired at different temperature; (e) *in vitro* release of free drug (TAC, blue line), TIF-Gel-TAC (black line) and in the presence of lipase (green line); (f) *ex vivo* release of free drug (TAC, blue line) and TIF-Gel-TAC in HEPES buffer (black line). Results in panels b, c, e and f are reported as mean  $\pm$  STDV (n=3).

#### Effect of the TOFA/TIF-Gel on dextran sulfate sodium (DSS)-induced acute colitis



To test the potential efficacy of the gel in treating an acute UC flare-up, we applied TIF-Gel loaded with TOFA to a mouse model of acute colitis induced by dextran sulfate sodium (DSS). DSS is toxic to epithelial cells and its application compromises the integrity of the intestinal barrier, thereby leading to an erosion of the epithelium and activation of submucosal immune cells by intestinal microbes (57). Through experimentation, we determined that bi-daily application of the gel yielded robust mitigation of local and systemic inflammation.

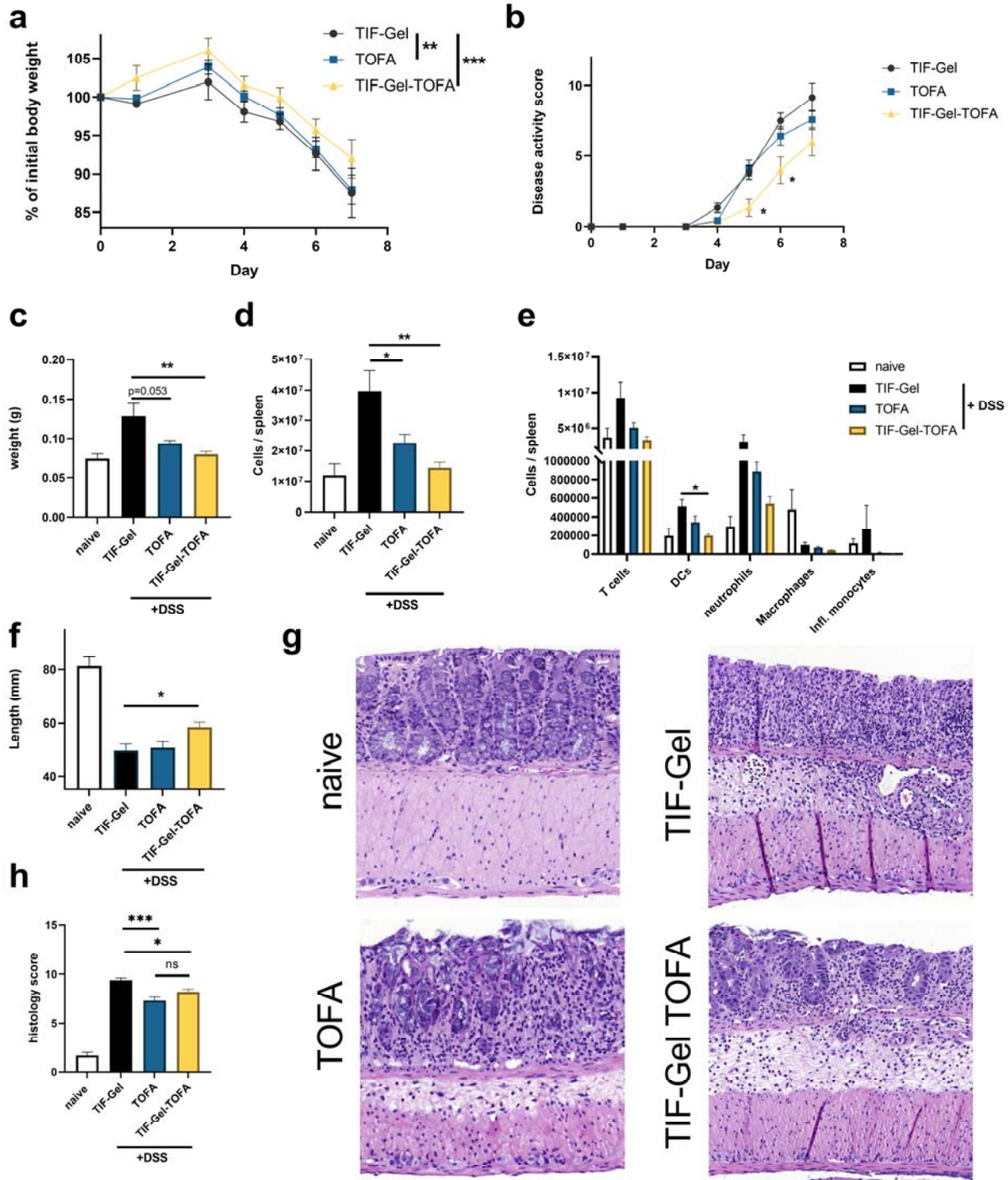


**Figure 3:** TIF-Gel-TOFA effectively mitigates intestinal inflammation and disease induced by DSS treatment in mice. Mice were prophylactically treated rectally with either empty gel (TIF-Gel), tofacitinib in vehicle (TOFA), or TOFA loaded-gel (TIF-Gel-TOFA) and thereafter challenged with 2% DSS in the drinking water. Treatments were then applied every other day until the end of the experiment. Weights (A) and disease score (B) were recorded throughout the experiment. At the end of the experiment, spleens, mesenteric lymph nodes (mLNs) and colons were removed from the mice. The spleens were weighed (C) and single splenocytes were enumerated (D). The frequencies of various splenic immune cell populations were determined by flow cytometry and total numbers calculated using the spleen cellularity determination (E). The mouse colon length was measured (F), and the colon was opened transversally, cleaned, and prepared for histology (G). Colon histopathology scores were determined and aggregated (H). \*:  $p < 0.05$ , \*\*:  $p < 0.01$ , \*\*\*:  $p < 0.001$  as determined by 2-way ANOVA (A), multiple Student's- tests with Holm-Sidak correction for multiple comparisons (B & E), and one way ANOVA with multiple comparisons and Tukey correction (C, D, F, H). All tests were performed using Prism (GraphPad) and applying default settings for the above-mentioned analyses; naïve values were excluded from analyses; all error bars are  $\pm$ SEM.

Mice treated with this regimen of TIF-Gel-TOFA displayed decreased weight loss and disease severity when compared to mice treated with an empty TIF-Gel (**Figures 3a** and **3b**). In contrast, drug in vehicle solution (TOFA), while improving weight loss, did not improve the disease score in these mice (**Figure 3b**). Of note, daily application of the compounds did not yield as robust results, and the differences between free TOFA and TIF-Gel-TOFA were less apparent under this regimen (**Figure S4**).

Signs of systemic inflammation, determined by spleen size and cellularity, were also alleviated in mice treated bi-daily with the TIF-Gel-TOFA (**Figures 3c** and **3d**). Furthermore, the total number of dendritic cells (DCs) present in the spleen was corrected to naïve levels by treatment with TIF-Gel-TOFA (**Figure 3e**). Local inflammation was also mitigated by the TIF-Gel-TOFA as determined by a reduction in colon shortening and pathology (**Figures 3f, 3g, and 3h**). For colon shortening, but not for histopathology, TIF-Gel-TOFA was more effective than the drug in vehicle, where differences were detectable in the proportion of immune cell populations of the spleens or mesenteric lymph nodes of the different treatment groups (**Figure S5**). Overall, these data indicate that a topically applied temperature-dependent *in situ*-forming gel carrying TOFA represents a valuable tool to mitigate acute intestinal inflammation.

### **Effect of the TIF-Gel-TOFA on T-cell transfer colitis**

TIF-Gel acts as a platform able to host and release molecules with different polarities (See Figure 2). Thus, we assessed the ability of the TIF-Gel loaded with the hydrophobic drug TAC to reduce colitis severity using a model of T cell-mediated colitis, namely the T cell transfer colitis model (58). In this model, naïve CD4 + T cells are transferred into B and T cell-deficient *Rag*<sup>-/-</sup> recipient mice, which results in the development of T helper cells that react against luminal antigens and subsequently induce a strong colon inflammation (59–61). Three days after naïve T cell transfer into *Rag*<sup>-/-</sup> hosts, mice were treated with 100  $\mu$ L i) TAC-loaded TIF-Gel (TIF-Gel-TAC), ii) empty TIF-Gel (TIF-Gel) or iii) TAC in vehicle solution (TAC) via daily rectal instillation (**Figure 4a**). Weight development and monitoring of disease activity demonstrated that mice that received empty TIF-Gel or TAC in vehicle solution started to develop the first signs of colitis around day 10 post T cell transfer as evidenced by



progressive weight loss and signs of diarrhoea (**Figures 4b** and **4c**). Of note, mice that were treated with TIF-Gel-TAC did not lose weight and diarrhoea scores were lower than in the other two groups (**Figures 4b** and **4c**). Moreover, all mice receiving TAC (either in TIF-Gels or administered in vehicle) showed longer colons and reduced spleen weight (**Figure 4d**), indicating reduced disease in these two groups when compared to mice treated with empty TIF-Gels.

On day 19 after T cell transfer, all mice were subjected to colonoscopy to evaluate macroscopic signs of colitis. Interestingly, TAC-administration via TIF-Gels as well as TAC administration in vehicle reduced endoscopic signs of colitis. Although there was a clear trend towards further reduction of endoscopic scores in mice that received TIF-Gel-TAC, this was not significant (**Figure 4e**). In contrast, and in line with disease activity scores, mice that received TIF-Gel-TAC did not only show clearly reduced colitis severity when compared to mice that were treated with empty TIF-Gels, but also when compared to mice that received TAC in vehicle solution (see histology score; **Figure 4e**). Taken together, these data clearly indicate that TAC administration via TIF-Gels is superior in reducing colitis severity than TAC-administration in vehicle.

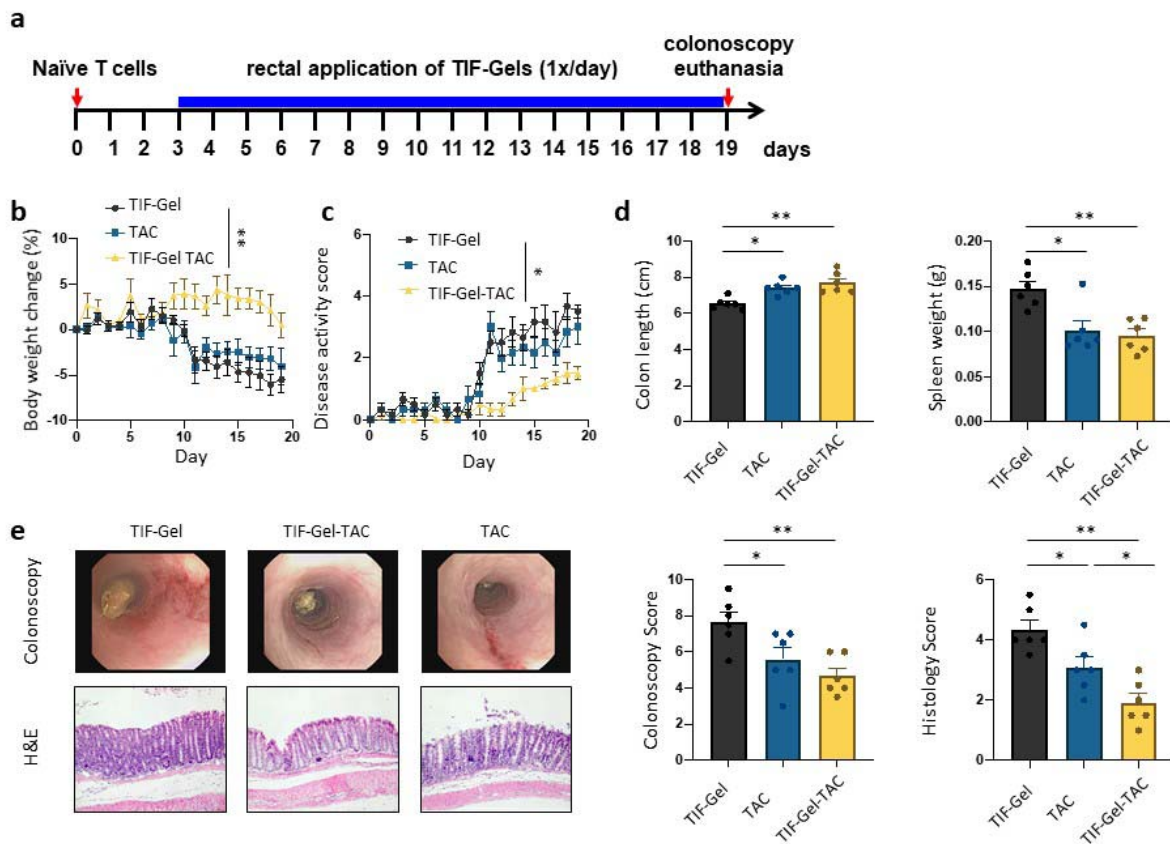


**Figure 4.** Assessment of the effect of TAC-loaded TIF-Gel on T cell-mediated colitis: 12–15-week-old *Rag*<sup>-/-</sup> mice develop colitis via transfer of  $2.5 \times 10^5$  naïve CD4<sup>+</sup> T cells. Starting on day 3 after T cell transfer, mice received daily rectal instillations with TIF-Gel without drug (TIF-Gel), TAC-loaded TIF-Gels (TIF-Gel-TAC) or TAC in vehicle (TAC). (a) Schematic overview on the experimental set-up; (b) weight development over the course of the

experiment; (c) cumulative disease activity score; (d) colon length and spleen weight; (e) representative pictures and respective scoring from mouse colonoscopy on day 19 post T cell transfer and from H&E-stained sections of the terminal colon collected on day 19 post T cell transfer. \* $p < 0.05$ , \*\* $p < 0.01$  as determined by 2-way ANOVA (b+c) and one way ANOVA with multiple comparisons and Tukey correction (d+e). All tests were performed using Prism (GraphPad) and applying default settings for the above-mentioned analyses; all error bars are  $\pm$ SEM.

T cell transfer colitis is mainly mediated by aberrantly activated T helper cells, and especially IFN- $\gamma$ <sup>+</sup> (Th1) and IL-17<sup>+</sup> (Th17) CD4<sup>+</sup> T cells contribute to the disease. To test the effect of TAC administration either in vehicle or in the TIF-Gels, we analysed proportions of T helper cells in the colonic lamina propria (**Figure 5a**), mesenteric lymph nodes (**Figure 5b**) and the spleen (**Figure 5c**). Of note, both TAC administration forms reduced the relative abundance of T cells in the *lamina propria*, mesenteric lymph nodes and the spleen (**Figures 5a-c**). Among those, Th1 and Th17 cells were reduced with TAC in vehicle as well as with TIF-Gel-TAG when compared to the mice that received empty TIF-Gels only (**Figure 5**). While there was no difference among Th1 cells between mice receiving of TAC in vehicle and those receiving TIF-Gel-TAC, the reduction in Th17 cells was significantly more pronounced in mice receiving TIF-Gel-TAC than in those receiving TAC in vehicle (**Figure 5**). In general, there was not much effect on the abundance of FoxP3<sup>+</sup> (regulatory) T cells (**Figure 5**). In summary, these results indicate that administration of TIF-Gel-TAC is superior in reducing disease-promoting T helper cells in the setting of T cell induced colitis.

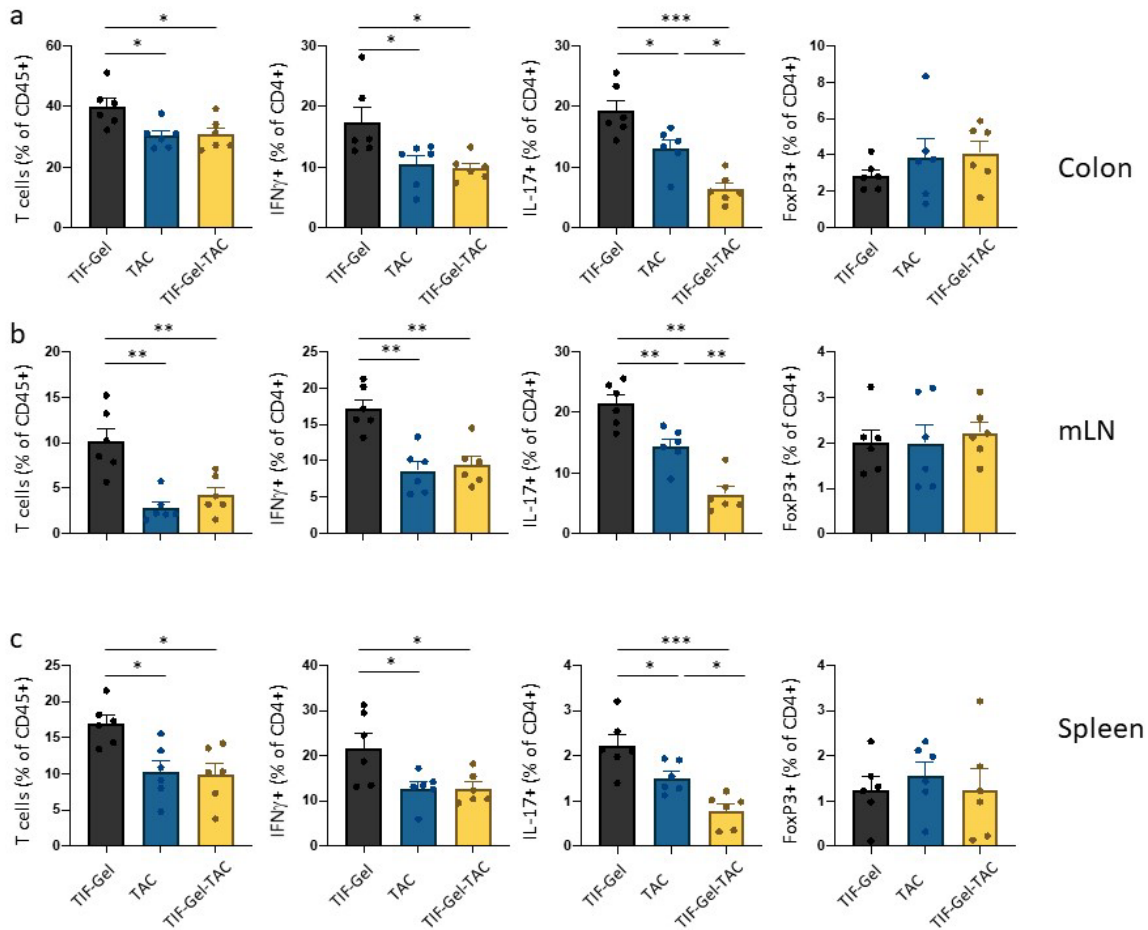


**Figure 5.** Immune cell populations in the colon from TAC-loaded TIF-Gel (TIF-Gel-TAC) treated mice: 12–15-week-old *Rag*<sup>-/-</sup> mice develop colitis via transfer of  $2.5 \times 10^5$  naïve T cells. Starting on day 3 post T cell transfer, mice received daily rectal instillations with TIF-Gel without drug (TIF-Gel), TAC-loaded TIF-Gels (TIF-Gel-TAC) or TAC in vehicle (TAC). Depicted are the relative abundance of the indicated cell populations in (a) the colonic *lamina propria*, (b) mesenteric lymph nodes; and (c) the spleen on day 19 after T cell transfer. \* $p < 0.05$ , \*\* $p < 0.01$ , \*\*\* $p < 0.001$  as determined by one way ANOVA with multiple comparisons and Tukey correction. All tests were performed using Prism (GraphPad) and applying default settings for the above-mentioned analyses; all error bars are  $\pm$ SEM.

## Discussion

The management of UC does not simply rely on the choice of a timely pharmacological treatment since the potential benefits of parenteral drug administration must always be weighed against recurring side effects due to systemic exposure to the drug (62). Thus, the specific localization of the disease should indeed encourage the pursuit of a rectal administration through which the drug directly reaches the site of inflammation with minimal systemic exposure (36). We demonstrated here that our newly developed TIF-Gel can host and release drugs of different polarity in a sustained manner, and the rectal temperature can be employed as stimulus to transform the plastic (and low viscosity) lamellar precursor into the structured (and high viscoelastic) cubic gel *in situ*. Hence, at 25 °C and in

the presence of 16% w/w percentage of water, MLO forms an L phase with a low structural strength resulting in a formulation that is easy to apply and able to reach more remote areas of the colon. On the other hand, the pseudoplastic precursor has a higher viscosity than commercially available enemas such as Asacol<sup>®</sup> and Pentasa<sup>®</sup> and foam-containing 5-ASA and budesonide; thus it can remain in the rectum for the time needed (at least 20 minutes) to avoid loss of material (39, 63, 64). Moreover, once applied to the rectum, the precursor L phase gradually absorbs heat (and the available amount of water) from the body and converts into the cubic phase, which forms the sustained release depot *in situ*. In comparison to the available liquid crystal technology<sup>®</sup> developed by the Swedish company Camurus (65, 66), which consists of an alcoholic lipid solution that transforms to a gel upon contact with water, TIF-gel is not only dependent on water content, but also uses temperature as a trigger for an *in situ* gelation. This aspect is of particular relevance since the volume of rectal fluid is low and highly affected by age, biological sex and pathology. In addition, TIF-gel is less fluid than a lipidic solution thereby avoiding a loss of material upon rectal application.

The validation of the gel efficacy to treat colitis was assessed in two different animal models, namely DSS-induced colitis and the T cell transfer colitis model. The dual approach was crucial to ascertain that the ability of our gel to treat the diseases is independent from the specific colitis trigger. DSS works through damaging the epithelial layer of the intestine, allowing for unfettered microbial-immune cell interactions and thereby results in acute and severe colitis mimicking acute disease flares observed in human ulcerative colitis (UC) (67). As topical TOFA has been applied to other inflammatory models (68), we postulated that this drug would be useful for testing the suitability of the TIF-Gel for application in the inflamed colon. Systemic and local inflammation were both reduced by the application of TOFA loaded into TIF-gel when compared to control DSS-challenged mice treated with empty gel or TOFA in vehicle solution. Interestingly, daily rectal administration of the drug in either form did not yield improved results, and reduced the differences between the gel-loaded and free drug, suggesting an enhanced time-release advantage of the drug when delivered as TIF-Gel-TOFA. Histopathological scores between the TIF-Gel and vehicle TOFA were similar, although by this time disease scores had normalized between the groups, and future studies with a less severe treatment regimen or altered time course (e.g. chronic low concentrations of DSS) might show more robust differences.

While DSS-induced colitis is mainly driven by the disruption of the intestinal epithelial barrier, the transfer colitis model is T cell-mediated; thus this model represents a different aspect of human IBD. In T cell transfer-mediated colitis, local administration of TAC using the TIF-Gel was superior in reducing colitis severity when compared to application of TAC in vehicle solution. This further confirms the results in the DSS model and supports the observation that the TIF-Gel represents a valid option to locally deliver drugs to the inflamed mucosa. Compared with other depot systems, our gel presents several potential advantages. First, TIF-Gel is made from a nontoxic, generally recognized as safe (GRAS) compound and, differently from other *in situ* forming implants (made by triglycerol monostearate or poly(lactic-co-glycolic acid), PLGA) currently in clinical trials or commercially available, it does not require organic solvents (that may be toxic) during its *in situ* formation. Moreover, the MLO is relatively inexpensive and available in large quantities at a high grade of purity (Good Manufacturing Practice or Food Grade); the manufacturing is a single-step process, and both tested drugs exhibit long-term stability once accommodated in the gel (see SI, Figure S3). All these conditions facilitate a straightforward transfer of the

technology from the bench to an industrial scale. Lastly, a low volume (0.1 mL) of TIF-Gel is able to deliver high amounts of drugs (up to 10 mg). Differently from the recently developed hydrogel for local drug delivery in IBD in which a low proportion of dexamethasone was encapsulated (53), our bulk gel is able to provide 100% drug loading (5 mg TOFA/100 mg gel and 1 mg TAC/100 mg gel) and still ensure a sustained release *in vitro*, *ex vivo* and *in vivo*. Moreover, 10% w/w of both TOFA and TAC can be loaded without affecting the phase identity and the transition temperature of the gel, which gives a lamellar phase at room temperature and a cubic (Ia3d) phase at 38 °C. These drug concentrations are higher than those contained in the commercially available enemas for UC treatment, which contain only 4% w/w of 5-ASA (in case of Asacol<sup>®</sup>) or 2% w/w of budesonide (for Budenofalk<sup>®</sup> and Entocort<sup>®</sup>). Taken together, in addition to making the manufacture of this gel formulation very efficient, administration of low volumes to the rectum may help in improving the patients' adherence to the therapy, a goal not always achieved because of the fecal urgency experienced as a consequence of the high volumes of daily applied enemas. Therefore, our formulation reduces not only the drug side effects associated with systemic therapy but also the drawbacks related to the use of the rectal formulations commercially available. In summary, our results demonstrate that TIF-Gel provides a valuable approach to effectively administer TOFA and TAC locally to the colonic mucosa resulting in sustained drug release. Furthermore, our findings suggest that the TIF-Gel enhances the localized activity of these anti-inflammatory drugs while potentially reducing the risk of side effects. Therefore, TIF-Gel would broaden the portfolio of the currently available platforms for topical therapies owing to a higher patient friendliness and a reduced leakage, while concomitantly decreasing problems with retention, bloating and urgency thus increasing the patient compliance to drug regimen.

### Study design

The goal of this study was to design a drug delivery system (TIF-Gel) for UC. We hypothesized that temperature could be used as a trigger to induce a formation of a viscous gel *in situ* and it should rapidly adhere to inflamed rectum mucosa and release its cargo. Firstly, we characterized the TIF-Gel *in vitro*; subsequently, we examined whether drugs delivery (TOFA and TAC) via TIF-Gel would affect therapeutic efficacy in two mouse models of UC, DSS-induced colitis and the mediated T cell model. Animals were randomly assigned to different treatment groups. For experiments, 6 mice were used per group. All animals were included in the analysis. Histopathology was analyzed by an experienced gastrointestinal pathologist blinded to group assignment using an established scoring system.

### Materials

Monolinolein (MLO) was purchased by NU-Check Prep, Inc. (MN, USA). Ultrapure water of resistivity 18.2 MΩ.cm was produced by Barnstead Smart2pure (Thermo scientific) and used as the aqueous phase. Methanol, acetonitrile, and tetrahydrofuran were analytical grade supplied by Fisher Scientific (Schwerte, Germany). Ethanol absolute >99.5 wt% was obtained from VWR chemicals BDH (London, UK). Tofacitinib citrate (TOFA) was purchased by LC laboratories (Woburn, MA) and tacrolimus (TAC) was obtained from R&S Pharmchem Co., Ltd (Shanghai, China). The lipase from porcine pancreas and methyl cellulose (viscosity 25 cp) were obtained from Sigma



Chemical Co. (St. Louis, USA). Caffeine (Ph. Eur. Quality) was purchased from Hanseler Swiss Pharma. HEPES salt was obtained from Carl Roth (Karlsruhe, Germany).

### **Gel preparation**

MLO was used as the lipid component of the mesophases and mixed with TOFA (5 % w/w; 5 mg/100 mg) or TAC (1% w/w; 1 mg/100 mg). Lipid/drug mixtures were prepared by dissolving the appropriate amounts of lipid and drug stock solutions together in ethanol. The solvent was then completely removed under reduced pressure (freeze-drying for 24 h at 0.22 mbar) and the dried lipid mixture was hydrated by mixing weighed amounts of water in sealed Pyrex tubes and alternatively centrifuging (10 min, 5000 g) several times at room temperature until a homogenous mixture was obtained. The mesophase was then equilibrated for 48 h at room temperature in the dark. For *in vivo* studies, after 48 h equilibration (as described above) the formulation was loaded into a 1-mL syringe (Injekt-F, Braun) and the dead volume of the animal feeding needle (20G, L × diam. 1.5 in. × 1.9 mm) for rectal administration was calculated so that exactly 100 mg was applied (see SI).

### **Small angle X-ray scattering**

SAXS measurements were used to determine the phase identity and symmetry of the produced LMPs. Measurements were performed on a Bruker AXS Micro, with a microfocused X-ray source, operating at voltage and filament current of 50 kV and 1000 μA, respectively. The Cu K $\alpha$  radiation ( $\lambda_{\text{Cu K}\alpha} = 1.5418 \text{ \AA}$ ) was collimated by a 2D Kratky collimator, and the data were collected by a 2D Pilatus 100K detector. The scattering vector  $Q = (4\pi/\lambda) \sin \theta$ , with  $2\theta$  being the scattering angle, was calibrated using silver behenate. Data were collected and azimuthally averaged using the Saxsgui software to yield 1D intensity vs. scattering vector  $Q$ , with a  $Q$  range from 0.001 to  $0.5 \text{ \AA}^{-1}$ . For all measurements, the samples were placed inside a stainless-steel cell between two thin replaceable mica sheets and sealed by an O-ring, with a sample volume of  $10 \text{ \mu L}$  and a thickness of  $\sim 1 \text{ mm}$ . Measurements were performed at 25, 30, 34, 36 and  $38 \text{ }^\circ\text{C}$ . Samples were equilibrated for 10 min before measurements whereas scattered intensity was collected over 30 min. On the other hand, for the kinetic study, the sample was pre equilibrated at  $25 \text{ }^\circ\text{C}$  and inserted in the sample holder kept at  $38 \text{ }^\circ\text{C}$  and the scattered intensity collected over 5 min. To determine the structural parameters such as the size of the water channels, SAXS data information on the lattice were combined with the composition of the samples (39).

### **Rheology experiments**

A stress-controlled rheometer (Modular Compact Rheometer MCR 72 from Anton Paar, Graz, Austria) was used in cone-plate geometry,  $0.993^\circ$  angle, and 49.942 mm diameter. The temperature control was set either at 25 or  $38 \text{ }^\circ\text{C}$ . First, a strain sweep was performed at 1 Hz between 0.002 and 100% strain to determine the linear range. Then, oscillatory frequency sweeps were performed at 0.1% strain between 0.1 and 100 rad/s. Frequency sweep measurements were performed at a constant strain in the linear viscoelastic regime (LVR), as determined by the oscillation strain sweep (amplitude sweep) measurement performed for each sample. Within the linear viscoelastic

region, in fact, the material response is independent of the magnitude of the deformation and the material structure is maintained intact; this is a necessary condition to accurately determine the mechanical properties of the material.

### **Release experiments: *in vitro* and *ex vivo* set-up and HPLC drug quantification.**

Formulations and free drug enema were tested *in vitro* and *ex vivo* with vertical diffusion cells (PermeGear, Pennsylvania, USA) using a 3000 nm polycarbonate membrane (Sterlitech Corporation, USA). HEPES buffer (8 mL) with a pH 7.4 or HEPES buffer enriched with 10% (v/v) of EtOH was used as the release medium for TOFA and TAC, respectively and the device was placed in a shaking incubator at 100 rpm and 37 °C. To investigate the effect of lipase on drug release, porcine pancreatic lipase (1000 U/mL,) was added to the sample in the donor chamber. *Ex vivo* experiments were performed using rat intestinal tissue to evaluate the drug release of our TIF-Gel. Briefly, fresh intestinal tissue was obtained and cut into suitable samples (2mm\*1mm\*1mm) for Franz cell apparatus. Tissue was placed on the polycarbonate membrane for tensile loading. At designated time points (0.5, 1, 1.5, 2, 3, 4, 5, 6, 7, 8 h), the release medium (HEPES buffer with a pH 7.4 in case of TOFA or HEPES buffer enriched with 30% (v/v) EtOH in case of TAC) was completely replaced with 8 mL of fresh medium, and 1 mL aliquot was taken for lyophilization. Each sample was resuspended with internal standard in the mobile phase and the drug content was analyzed by HPLC (details are reported in the SI). The same experimental design was used for both formulations. Moreover, samples of TIF-Gel containing drug were stored at room temperature and 4 °C for 30 days. The drug stability was determined by HPLC analysis. The same experimental design was used for both drugs.

### ***In vivo* investigation**

#### **Chemically induced colitis based on application of DSS**

Female 6-8 week-old C57B/6J mice were ordered from Charles River Germany and maintained under specific and opportunistic pathogen-free (SOPF) microbiota conditions at the animal facility of the University of Bern. Mice were ear-marked, randomly assigned to different cages and treatment groups, and bedding mixed between all cages to avoid potential cage effects on microbiota. All methods used were approved by the Bernese animal welfare authority (permission no. BE 20/18). One day prior to the start of DSS supplementation, mice were intra-rectally injected with 100 µL of empty gel, TOFA in 1% methylcellulose, or gel loaded with drug (5 mg /100 µL). The next day, drinking water was supplemented with 2% w/v dextran sodium sulfate (DSS; MP Biomedicals, 160110). Every other day, the different compounds were applied intra-rectally until the end of the experiment (See schematic, **Figure S4h**). During the experiment, the mice were constantly monitored and the weight and disease scores were recorded when appropriate. Disease score was determined by grading of 1-4 of the following criteria (with grade 4 corresponding to most unhealthy/abnormal): posture, mobility, fur appearance, weight, stool consistency, and stool color, as previously described (69). At the termination of the experiment, mice were euthanized by asphyxia with carbon dioxide, and organs were collected and used as described in the results. Swiss rolls (70) were made from the colons, fixed overnight with 10% formalin in PBS, then washed with PBS, embedded in paraffin, and sectioned with H&E staining. Histopathology scoring was performed by board-certified pathologist, in a blinded manner, using the following criteria: loss of goblet cells, crypt abscesses, epithelial erosions, hyperemia, thickness of mucosa, and cellular infiltration (maximal score for each criterion: 3)(71).

### **Flow cytometry and quantification of single cells**

The gating strategy was adapted from previously published work (72). Briefly, mouse spleens (after weighing) and mesenteric lymph nodes were homogenized through a 70 µm cell strainer, after which point the red blood cells were removed from the spleen by re-suspending the cell pellet in ACK lysing buffer (150mM NH<sub>4</sub>Cl, 10mM KHCO<sub>3</sub>, 0.1mM; pH: 7.4) at room temperature for 5 min. Splenocytes were quantified using a CASY cell counter (Omni Life Sciences) and the following populations were quantified following single cell and live/dead selection (Thermofischer, L34961). T cells (defined as CD3ε+ cells; antibody used: eBioscience, 25-0031-82); dendritic cells (CD11c+, CD11b+; Biolegend 117324 & 101241); neutrophils (CD11b+, Ly6G+; Biolegend, B156884), macrophages (CD11b+, CD11c-, Ly6G-, Ly6C-), and inflammatory monocytes (CD11b+, Ly6C+; Biolegend, 128024). Stained cells were analysed on a BD BioscienceLSR II SORP flow cytometer.

### **T-cell transfer colitis**

To induce T cell mediated colitis, CD4+ T cells were isolated from the spleen of C57/BL6 mice using the CD4 T cell isolation kit from Stemcell Technologies (# 19852; Cologne, Germany) and subsequently naïve T helper cells (CD3+, CD4+, CD25low, CD6Lhigh, CD44low cells) were sorted on a FACS Aria III (Becton Dickinson; Eysins, Switzerland) as described previously (54–56). 12-15 week-old male and female *Rag*<sup>-/-</sup> mice in the C57/BL6 background (originally purchased from Taconic from which a local colony was maintained in our vivarium) were injected intraperitoneally with 2.5 x10<sup>5</sup> naïve T helper cells. Mice (6 animals/group) were randomly assigned to different cages and treatment groups, and bedding mixed between all cages to avoid potential cage effects on microbiota. All methods used were approved by the animal welfare authority (permission no. ZH043/2021). Starting on day 3 post T cell injection, mice received rectal instillations (100 µL) of empty TIF-Gels, TAC-loaded TIG-Gels or TAC in vehicle solution (1% nitrocellulose in distilled water) once per day until the end of the experiment. Weight development and disease activity scores were measured on a daily basis. On the last day of the experiment (day 18), the mice were anaesthetized using a mixture of ketamine 90–120 mg/kg bodyweight (Vétoquinol, Bern, Switzerland) and xylazine 8 mg/kg bodyweight (Bayer, Lyssach, Switzerland) and subjected to mouse endoscopy to assess the extent of endoscopic colitis as described previously (61) using the following parameters: 1) thickening of the colon wall, 2) vascularization/bleeding, 3) extent of fibrin deposits, 4) granular appearance of the colon wall, 5) stool consistency. Each parameter was given a score from 0 (normal) to 3 (most severe appearance), resulting in a maximal total score of 15. After colonoscopy, the mice were sacrificed and colon tissue harvested for histology and isolation of *lamina propria* immune cells. Immune cells were isolated from the colon, mesenteric lymph nodes and the spleen, and analyzed for immune cell subsets as described previously (73).

### **H&E staining and histological analysis of colitis severity**

To assess the microscopic extent of colitis, formalin-fixed, paraffin embedded sections of the most distal 1.5 cm of the colon were subjected to hematoxylin and eosin (H&E) staining using standard protocols (61). The sections were analyzed by two blinded scientists for the extent of epithelial damage (score 0-4) and infiltration of immune cells (score 0-4) resulting in a maximal possible score of 8. Images were taken using a Zeiss Axio Imager.Z2 microscope

(Zeiss), equipped with an AxioCam HRc (Zeiss, Jena, Germany) camera and ZEN imaging software (Zeiss, Germany).

**Credit authorship contribution:**

MC: Investigation, Validation and Visualization (LMPs preparation, release experiments and rheology); Formal analysis, Data curation, Writing – original draft.

MRS: Investigation, Validation and Visualization; Writing – original draft

PL: Conceptualization; Supervision; Project administration; Funding acquisition; Writing - review & editing.

SA: Conceptualization; Data curation; Methodology; Validation; Formal analysis; Investigation; Writing - original draft; Visualization.

RM: Writing - review & editing

RAG: Investigation, Validation and Visualization, Writing – original draft, Formal analysis

AM: Formal analysis

PK: Conceptualization; Supervision; Project administration; Funding acquisition; Writing - review & editing

GR: Conceptualization; Supervision; Project administration; Funding acquisition; Writing - review & editing

All authors discussed the results and commented on the manuscript.

**Declaration of Competing Interest.**

The authors declare that they have no known competing financial interests or personal relationships that could have appeared to influence the work reported in this paper.

**Acknowledgments.**

Dr. Serena Rosa Alfarano and Ms. Francesca Victorelli (Laboratory of Food & Soft Materials, Institute of Food, Nutrition and Health, IFNH; Department for Health Sciences and Technology, D-HEST, ETH Zurich Switzerland) are kindly acknowledged for their precious support during the SAXS experiments. We thank the team of the Translational Research Unit of the Institute of Pathology. The authors gratefully acknowledge the Innovation Office of the University of Bern for the financial support of the *in vivo* study.

PK is supported by grants from the Swiss National Science Foundation (310030\_189185) and by The Bern University Research Foundation. RAG received funding from a “Seal of Excellence Fund” (SELF) from the University of Bern.

**REFERENCES**

1. J. Meier, in *Inflammatory Bowel Disease Nursing Manual*, (Springer International Publishing, Cham, 2019), pp. 11–14.
2. R. Ungaro, S. Mehandru, P. B. Allen, L. Peyrin-Biroulet, J. F. Colombel, Ulcerative colitis *Lancet* **389**, 1756–1770 (2017).
3. S. Singh, J. R. Allegretti, S. M. Siddique, J. P. Terdiman, AGA Technical Review on the Management of

- Moderate to Severe Ulcerative Colitis, *Gastroenterology* **158**, 1465-1496.e17 (2020).
4. C. W. Ko, S. Singh, J. D. Feuerstein, C. Falck-Ytter, Y. Falck-Ytter, R. K. Cross, S. Crockett, J. Feuerstein, S. Flamm, J. Inadomi, C. Ko, T. Muniraj, R. O'Shea, J. Pandolfino, A. Patel, R. Sharaf, S. Siddique, G. Su, K. Wang, A. Weizman, AGA Clinical Practice Guidelines on the Management of Mild-to-Moderate Ulcerative Colitis, *Gastroenterology* **156**, 748–764 (2019).
  5. M. Manz, P. Michetti, F. Seibold, G. Rogler, C. Beglinger, Treatment algorithm for moderate to severe ulcerative colitis *Swiss Med. Wkly.* **141** (2011), doi:10.4414/smw.2011.13235.
  6. J. Wehkamp, E. F. Stange, Recent advances and emerging therapies in the non-surgical management of ulcerative colitis, *F1000Research* **7**, 1207 (2018).
  7. R. Khanna, W. Afif, Ustekinumab for Ulcerative Colitis *Gastroenterology* **160**, 2184–2186 (2021).
  8. W. J. Sandborn, B. G. Feagan, G. D'Haens, D. C. Wolf, I. Jovanovic, S. B. Hanauer, S. Ghosh, A. Petersen, S. Y. Hua, J. H. Lee, L. Charles, D. Chitkara, K. Usiskin, J.-F. Colombel, L. Laine, S. Danese, Ozanimod as Induction and Maintenance Therapy for Ulcerative Colitis, *N. Engl. J. Med.* **385**, 1280–1291 (2021).
  9. G. D'Haens, Risks and benefits of biologic therapy for inflammatory bowel diseases, *Gut* **56**, 725–732 (2007).
  10. S. Ben-Horin, R. Mao, M. Chen, Optimizing biologic treatment in IBD: objective measures, but when, how and how often?, *BMC Gastroenterol.* **15**, 178 (2015).
  11. J. Kirchgesner, M. Lemaitre, F. Carrat, M. Zureik, F. Carbonnel, R. Dray-Spira, Risk of Serious and Opportunistic Infections Associated With Treatment of Inflammatory Bowel Diseases, *Gastroenterology* **155**, 337-346.e10 (2018).
  12. G. Mocchi, M. Marzo, A. Papa, A. Armuzzi, L. Guidi, Dermatological adverse reactions during anti-TNF treatments: Focus on inflammatory bowel disease *J. Crohn's Colitis* **7**, 769–779 (2013).
  13. F. Hoentjen, A. A. van Bodegraven, Safety of anti-tumor necrosis factor therapy in inflammatory bowel disease *World J. Gastroenterol.* **15**, 2067–2073 (2009).
  14. S. Danese, M. Grisham, J. Hodge, J.-B. Telliez, JAK inhibition using tofacitinib for inflammatory bowel disease treatment: a hub for multiple inflammatory cytokines, *Am. J. Physiol. Liver Physiol.* **310**, G155–G162 (2016).
  15. S. Bonovas, T. Lytras, G. Nikolopoulos, L. Peyrin-Biroulet, S. Danese, Systematic review with network meta-analysis: comparative assessment of tofacitinib and biological therapies for moderate-to-severe ulcerative colitis *Aliment. Pharmacol. Ther.* (2018), doi:10.1111/apt.14449.
  16. S. Singh, M. Fumery, W. J. Sandborn, M. H. Murad, Systematic review with network meta-analysis: first- and second-line pharmacotherapy for moderate-severe ulcerative colitis *Aliment. Pharmacol. Ther.* (2018), doi:10.1111/apt.14422.
  17. H. Ogata, T. Matsui, M. Nakamura, M. Iida, M. Takazoe, Y. Suzuki, T. Hibi, A randomised dose-finding study of oral tacrolimus (FK506) therapy in refractory ulcerative colitis, *Gut* **55**, 1255–1262 (2006).
  18. G. Rogler, Gastrointestinal and liver adverse effects of drugs used for treating IBD, *Best Pract. Res. Clin. Gastroenterol.* (2010), doi:10.1016/j.bpg.2009.10.011.
  19. R. Westhovens, Clinical efficacy of new JAK inhibitors under development. Just more of the same?, *Rheumatol. (United Kingdom)* **58**, i27–i33 (2019).
  20. K. Haga, T. Shibuya, K. Nomura, K. Okahara, O. Nomura, D. Ishikawa, N. Sakamoto, T. Osada, A. Nagahara,



- Effectiveness and Nephrotoxicity of Long-Term Tacrolimus Administration in Patients with Ulcerative Colitis, *J. Clin. Med.* **9**, 1771 (2020).
21. S. Godat, N. Fournier, E. Safroneeva, P. Juillerat, A. Nydegger, A. Straumann, S. Vavricka, L. Biedermann, T. Greuter, M. Fraga, K. Abdelrahman, D. Hahnloser, B. Sauter, G. Rogler, P. Michetti, A. M. Schoepfer, Frequency and type of drug-related side effects necessitating treatment discontinuation in the Swiss Inflammatory Bowel Disease Cohort, *Eur. J. Gastroenterol. Hepatol.* **30**, 612–620 (2018).
  22. P. Frei, L. Biedermann, C. N. Manser, M. Wilk, M. Manz, S. R. Vavricka, G. Rogler, Topical therapies in inflammatory bowel disease, *Digestion* **86**, 36–44 (2012).
  23. R. D. Cohen, R. Weisshof, A comprehensive review of topical therapies for distal ulcerative colitis, *Gastroenterol. Hepatol.* **16**, 21–27 (2020).
  24. J. K. MARSHALL, E. J. IRVINE, Rectal aminosalicilate therapy for distal ulcerative colitis: a meta-analysis *Aliment. Pharmacol. Ther.* **9**, 293–300 (1995).
  25. S. Katz, G. R. Lichtenstein, M. A. Safdi, in *Gastroenterology and Hepatology*, (Millenium Medical Publishing, 2010), vol. 6, pp. 1–12.
  26. M. Safdi, M. DeMicco, C. Sninsky, P. Banks, L. Wruble, J. Deren, G. Koval, T. Nichols, S. Targan, C. Fleishman, A Double-Blind Comparison of Oral versus Rectal Mesalamine versus Combination Therapy in the Treatment of Distal Ulcerative Colitis., *Am. J. Gastroenterol.* **92** (1997).
  27. I. C. Lawrance, T. S. Copeland, Rectal tacrolimus in the treatment of resistant ulcerative proctitis, *Aliment. Pharmacol. Ther.* **28**, 1214–1220 (2008).
  28. J. M. van Dieren, A. A. van Bodegraven, E. J. Kuipers, E. N. Bakker, A. C. Poen, H. van Dekken, E. E. S. Nieuwenhuis, C. J. van der Woude, Local application of tacrolimus in distal colitis: Feasible and safe, *Inflamm. Bowel Dis.* **15**, 193–198 (2009).
  29. I. C. Lawrance, A. Baird, D. Lightower, G. Radford-Smith, J. M. Andrews, S. Connor, Efficacy of Rectal Tacrolimus for Induction Therapy in Patients With Resistant Ulcerative Proctitis, *Clin. Gastroenterol. Hepatol.* **15**, 1248–1255 (2017).
  30. S. R. Fehily, F. C. Martin, M. A. Kamm, Simple water-based tacrolimus enemas for refractory proctitis, *JGH Open* **4**, 561–564 (2020).
  31. I. C. Lawrance, A. Baird, D. Lightower, G. Radford-Smith, J. M. Andrews, S. Connor, Efficacy of Rectal Tacrolimus for Induction Therapy in Patients With Resistant Ulcerative Proctitis, *Clin. Gastroenterol. Hepatol.* (2017), doi:10.1016/j.cgh.2017.02.027.
  32. I. Seoane-Viaño, J. J. Ong, A. Luzardo-Álvarez, M. González-Barcia, A. W. Basit, F. J. Otero-Espinar, A. Goyanes, 3D printed tacrolimus suppositories for the treatment of ulcerative colitis, *Asian J. Pharm. Sci.* **16**, 110–119 (2021).
  33. P. Frei, G. Rogler, Rectal treatment for inflammatory bowel disease, (2017).
  34. P. Gionchetti, F. Rizzello, A. Venturi, C. Brignola, M. Ferretti, S. Peruzzo, M. Campieri, Comparison of mesalazine suppositories in proctitis and distal proctosigmoiditis, *Aliment. Pharmacol. Ther.* **11**, 1053–1057 (1997).
  35. M. Campieri, P. Gionchetti, A. Belluzzi, C. Brignola, G. M. Tabanelli, M. Miglioli, L. Barbara, 5-Aminosalicilic acid as enemas or suppositories in distal ulcerative colitis?, *J. Clin. Gastroenterol.* **10**, 406–409 (1988).

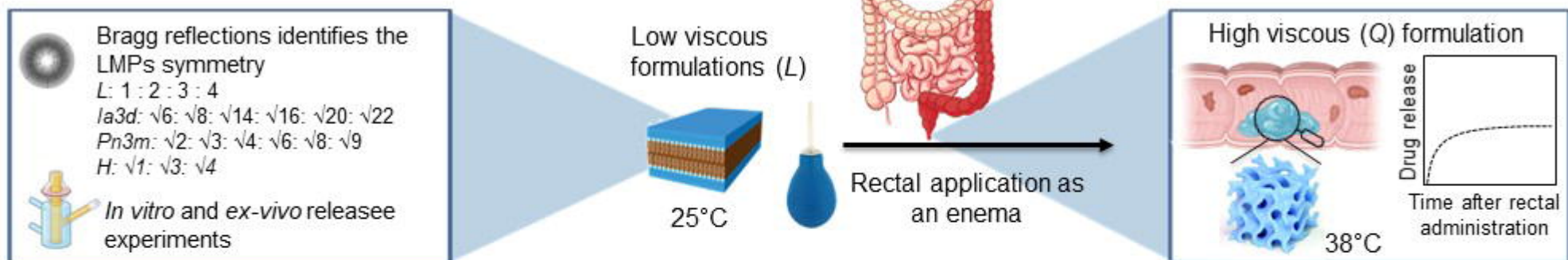
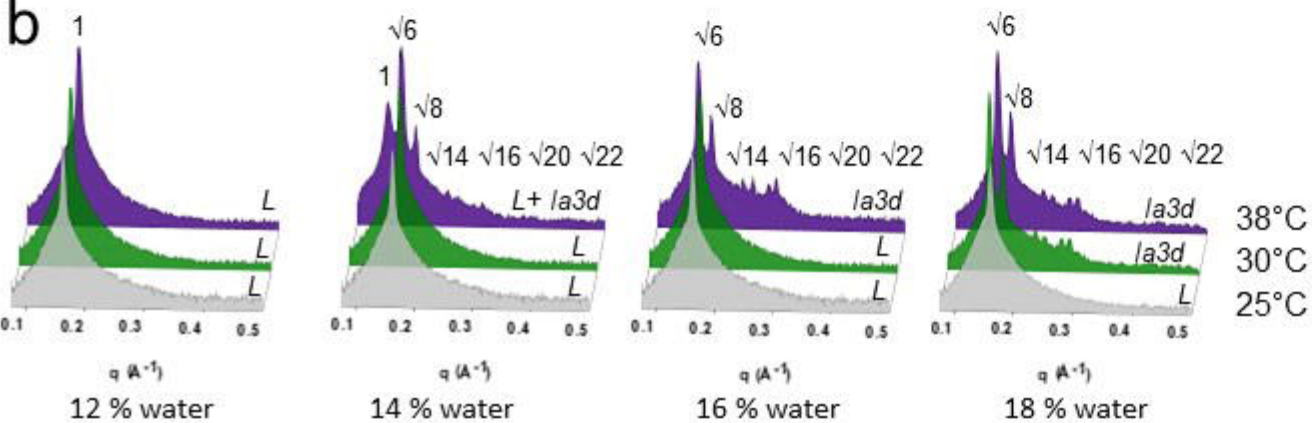
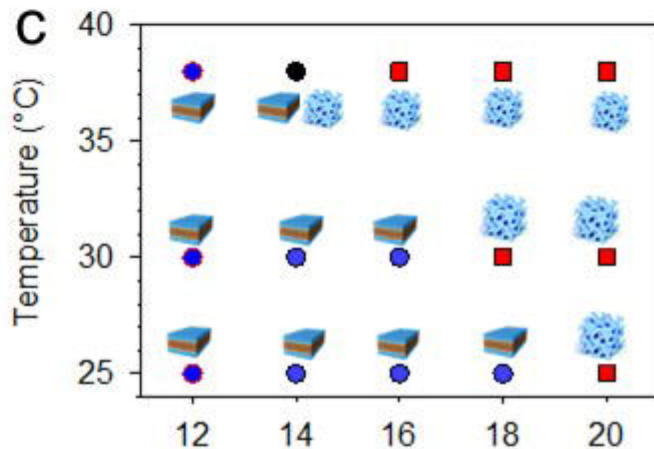
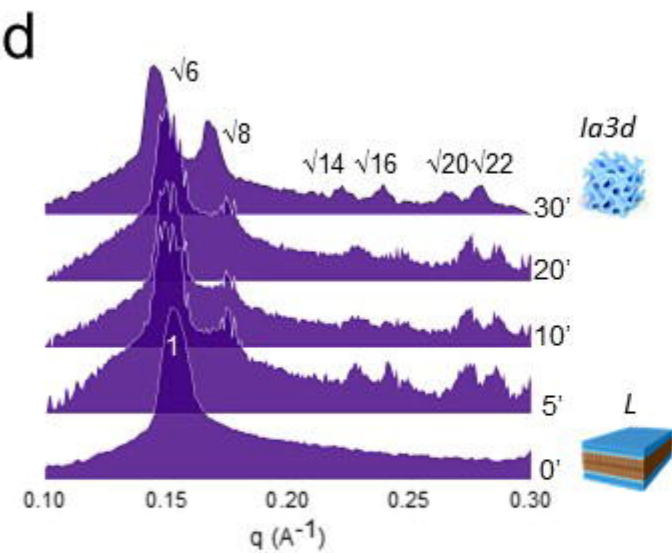
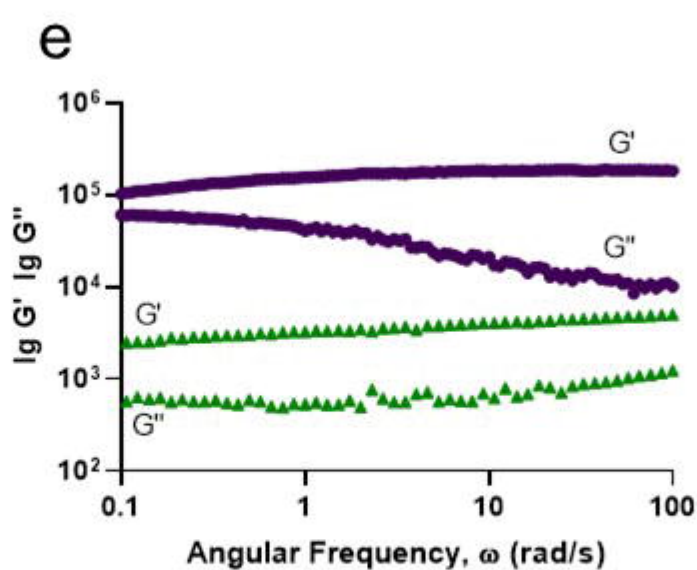
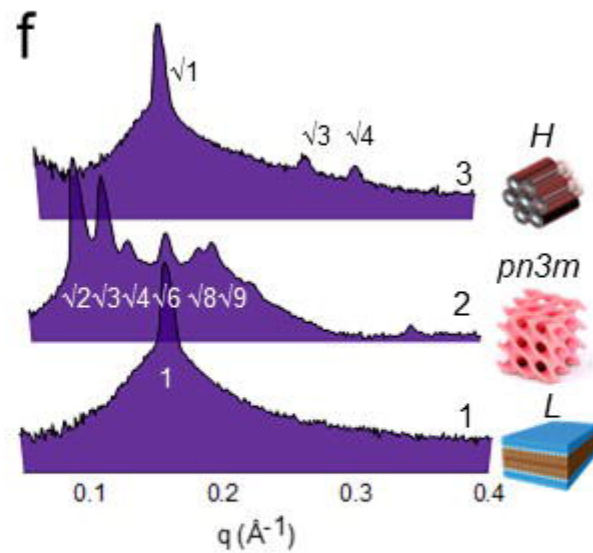
36. F. Seibold, N. Fournier, C. Beglinger, C. Mottet, V. Pittet, G. Rogler, Topical therapy is underused in patients with ulcerative colitis, *J. Crohn's Colitis* **8**, 56–63 (2014).
37. Nidhi, M. Rashid, V. Kaur, S. S. Hallan, S. Sharma, N. Mishra, Microparticles as controlled drug delivery carrier for the treatment of ulcerative colitis: A brief review *Saudi Pharm. J.* **24**, 458–472 (2016).
38. S. Aleandri, R. Mezzenga, The physics of lipidic mesophase delivery systems, *Phys. Today* **73**, 38–44 (2020).
39. R. Mezzenga, C. Meyer, C. Servais, A. I. Romoscanu, L. Sagalowicz, R. C. Hayward, Shear rheology of lyotropic liquid crystals: a case study, *Langmuir* **21**, 3322–3333 (2005).
40. W. K. Fong, T. Hanley, B. J. Boyd, Stimuli responsive liquid crystals provide “on-demand” drug delivery in vitro and in vivo, *J Control Release* **135**, 218–226 (2009).
41. A. Tardieu, V. Luzzati, Polymorphism of lipids a novel cubic phase - a cage-like network of rods with enclosed spherical micelles, *Biochim Biophys Acta* **219**, 11–17 (1970).
42. M. Camilleri, D. R. Linden, Measurement of Gastrointestinal and Colonic Motor Functions in Humans and Animals *CMGH* **2**, 412–428 (2016).
43. S. Wirtz, M. F. Neurath, Mouse models of inflammatory bowel disease *Adv. Drug Deliv. Rev.* **59**, 1073–1083 (2007).
44. R. Eri, M. A. McGuckin, R. Wadley, T cell transfer model of colitis: A great tool to assess the contribution of T cells in chronic intestinal inflammation, *Methods Mol. Biol.* **844**, 261–275 (2012).
45. D. Demurtas, P. Guichard, I. Martiel, R. Mezzenga, C. Hébert, L. Sagalowicz, Direct visualization of dispersed lipid bicontinuous cubic phases by cryo-electron tomography, *Nat. Commun.* **6** (2015), doi:10.1038/ncomms9915.
46. N. Rahanyan-Kagi, S. Aleandri, C. Speziale, R. Mezzenga, E. M. Landau, Stimuli-responsive lipidic cubic phase: triggered release and sequestration of guest molecules, *Chemistry (Easton)*. **21**, 1873–1877 (2015).
47. Q. Liu, Y. Xiao, A. Hawley, B. J. Boyd, Lipid-based lyotropic liquid crystalline phase transitions as a novel assay platform using birefringence as the visual signal output, *J. Mater. Chem. B* **8**, 6277–6285 (2020).
48. C. H. Salamanca, A. Barrera-Ocampo, J. C. Lasso, N. Camacho, C. J. Yarce, Franz diffusion cell approach for pre-formulation characterisation of ketoprofen semi-solid dosage forms, *Pharmaceutics* **10** (2018), doi:10.3390/pharmaceutics10030148.
49. R. A. Rocha, D. Vélez, V. Devesa, In vitro evaluation of intestinal fluoride absorption using different cell models, *Toxicol. Lett.* (2012), doi:10.1016/j.toxlet.2012.02.015.
50. G. Nollevaux, C. Devillé, B. El Moualij, W. Zorzi, P. Deloyer, Y.-J. Schneider, O. Peulen, G. Dandrifosse, Development of a serum-free co-culture of human intestinal epithelium cell-lines (Caco-2/HT29-5M21), *BMC Cell Biol.* **7**, 20 (2006).
51. E. Walter, S. Janich, B. J. Roessler, J. M. Hilfinger, G. L. Amidon, HT29-MTX/Caco-2 Cocultures as an in Vitro Model for the Intestinal Epithelium: In Vitro-in Vivo Correlation with Permeability Data from Rats and Humans, *J. Pharm. Sci.* **85**, 1070–1076 (1996).
52. D. Low, D. D. Nguyen, E. Mizoguchi, Drug Design, Development and Therapy Dovepress Animal models of ulcerative colitis and their application in drug research, *Drug Des. Devel. Ther.* (2013), doi:10.2147/DDDT.S40107.
53. D. Low, D. D. Nguyen, E. Mizoguchi, Animal models of ulcerative colitis and their application in drug research *Drug Des. Devel. Ther.* **7**, 1341–1356 (2013).

54. N. A. Ivanova, A. Trapani, C. Di Franco, D. Mandracchia, G. Trapani, C. Franchini, F. Corbo, G. Tripodo, I. N. Kolev, G. S. Stoyanov, K. Z. Bratoeva, In vitro and ex vivo studies on diltiazem hydrochloride-loaded microsponges in rectal gels for chronic anal fissures treatment, *Int. J. Pharm.* (2019), doi:10.1016/j.ijpharm.2018.12.039.
55. S. Zhang, J. Ermann, M. D. Succi, A. Zhou, M. J. Hamilton, B. Cao, J. R. Korzenik, J. N. Glickman, P. K. Vemula, L. H. Glimcher, G. Traverso, R. Langer, J. M. Karp, An inflammation-targeting hydrogel for local drug delivery in inflammatory bowel disease, *Sci. Transl. Med.* **7**, 1–11 (2015).
56. R. Eliakim, Z. Tulassay, L. Kupcinskis, K. Adamonis, J. Pokrotnieks, S. Bar-Meir, A. Lavy, R. Mueller, R. Greinwald, I. Chermesh, V. Gross, Clinical trial: Randomized-controlled clinical study comparing the efficacy and safety of a low-volume vs. a high-volume mesalazine foam in active distal ulcerative colitis, *Aliment. Pharmacol. Ther.* **26**, 1237–1249 (2007).
57. S. Wirtz, V. Popp, M. Kindermann, K. Gerlach, B. Weigmann, S. Fichtner-Feigl, M. F. Neurath, Chemically induced mouse models of acute and chronic intestinal inflammation, *Nat. Protoc.* **12**, 1295–1309 (2017).
58. D. V. Ostanin, J. Bao, I. Koboziev, L. Gray, S. A. Robinson-Jackson, M. Kosloski-Davidson, V. H. Price, M. B. Grisham, T cell transfer model of chronic colitis: Concepts, considerations, and tricks of the trade *Am. J. Physiol. - Gastrointest. Liver Physiol.* **296**, 135–146 (2009).
59. M. R. Spalinger, S. Kasper, C. Chassard, T. Raselli, I. Frey-Wagner, C. Gottier, S. Lang, K. Atrott, S. R. Vavricka, F. Mair, B. Becher, C. Lacroix, M. Fried, G. Rogler, M. Scharl, PTPN2 controls differentiation of CD4+ T cells and limits intestinal inflammation and intestinal dysbiosis, *Mucosal Immunol.* **8**, 918–929 (2015).
60. M. R. Spalinger, M. Schwarzfischer, A. Niechcial, K. Atrott, A. Laimbacher, C. Gottier, S. Lang, M. Scharl, Loss of PTPN22 Promotes Intestinal Inflammation by Compromising Granulocyte-mediated Antibacterial Defence, *J. Crohn's Colitis* **15**, 2118–2130 (2021).
61. M. R. Spalinger, T. S. B. Schmidt, M. Schwarzfischer, L. Hering, K. Atrott, S. Lang, C. Gottier, A. Geirnaert, C. Lacroix, X. Dai, D. J. Rawlings, A. C. Chan, C. von Mering, G. Rogler, M. Scharl, Protein tyrosine phosphatase non-receptor type 22 modulates colitis in a microbiota-dependent manner, *J. Clin. Invest.* **129**, 2527–2541 (2019).
62. T. Raine, S. Bonovas, J. Burisch, T. Kucharzik, M. Adamina, V. Annese, O. Bachmann, D. Bettenworth, M. Chaparro, W. Czuber-Dochan, P. Eder, P. Ellul, C. Fidalgo, G. Fiorino, P. Gionchetti, J. P. Gisbert, H. Gordon, C. Hedin, S. Holubar, M. Iacucci, K. Karmiris, K. Katsanos, U. Kopylov, P. L. Lakatos, T. Lytras, I. Lyutakov, N. Noor, G. Pellino, D. Piovani, E. Savarino, F. Selvaggi, B. Verstockt, A. Spinelli, Y. Panis, G. Doherty, ECCO Guidelines on Therapeutics in Ulcerative Colitis: Medical Treatment, *J. Crohns. Colitis* **16**, 2–17 (2022).
63. M. H. Otten, G. de Haas, R. van den Ende, Colonic range of 5-ASA enemas in healthy individuals, with a comparison of their physical and chemical characteristics. An open, single-dose, randomized, cross-over study, *Aliment. Pharmacol. Ther.* **11**, 693–697 (1997).
64. J. R. Ingram, Comparative study of enema retention and preference in ulcerative colitis, *Postgrad. Med. J.* **81**, 594–598 (2005).
65. F. Tiberg, I. Harwigsson, M. Johnsson, High bioavailability opioid formulations US 2013/0190341 A1, *US Pat. App.* 13/558, 463 **1** (2013) (available at <https://patents.google.com/patent/US20130190341A1/en>).
66. P. Examiner, V. Bali, ( 12 ) United States Patent ( 10 ) Patent No. : See application file for complete search history, **2**, 1–6 (2006).

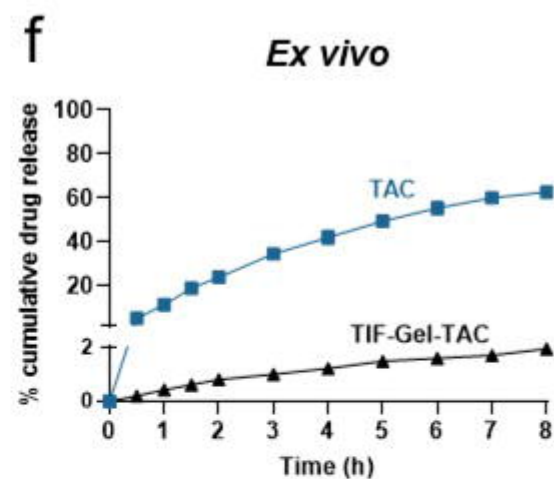
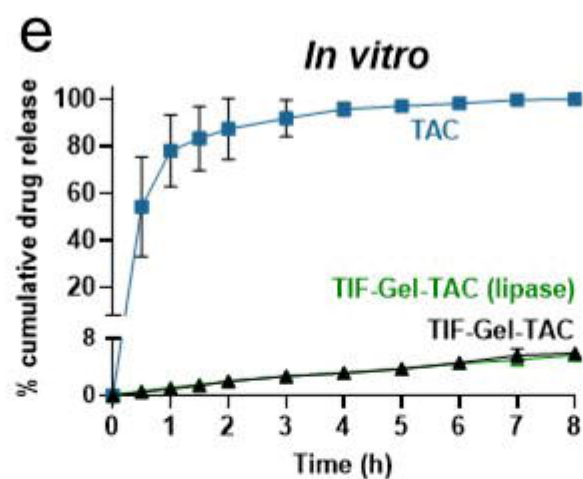
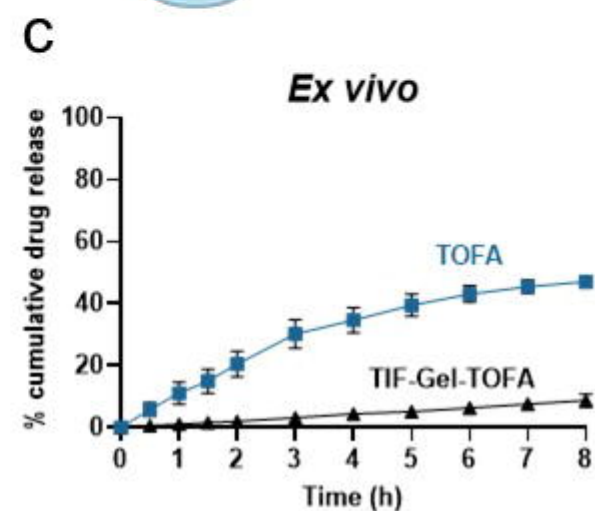
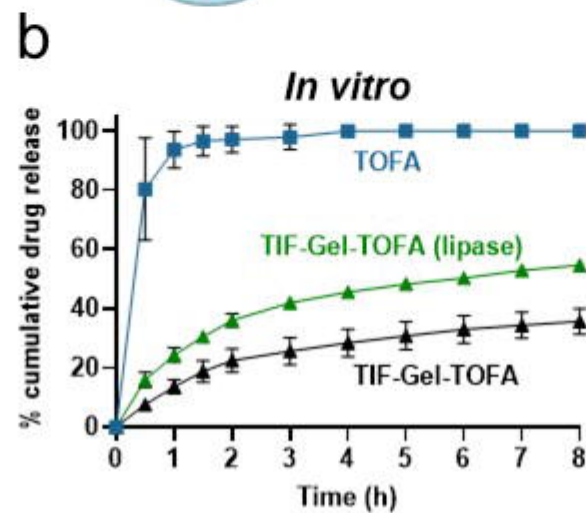
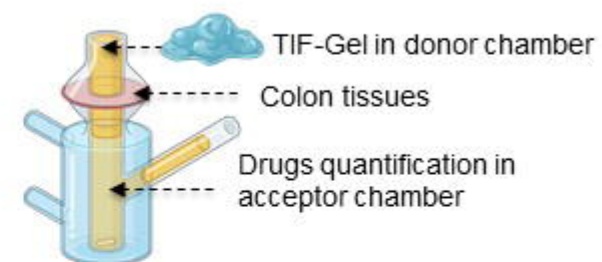
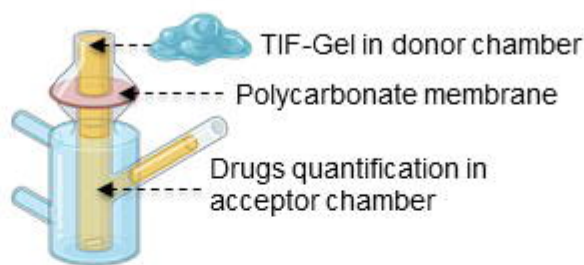
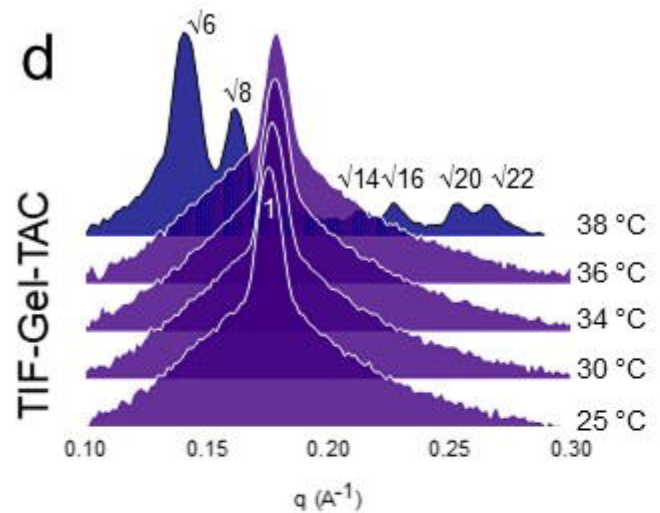
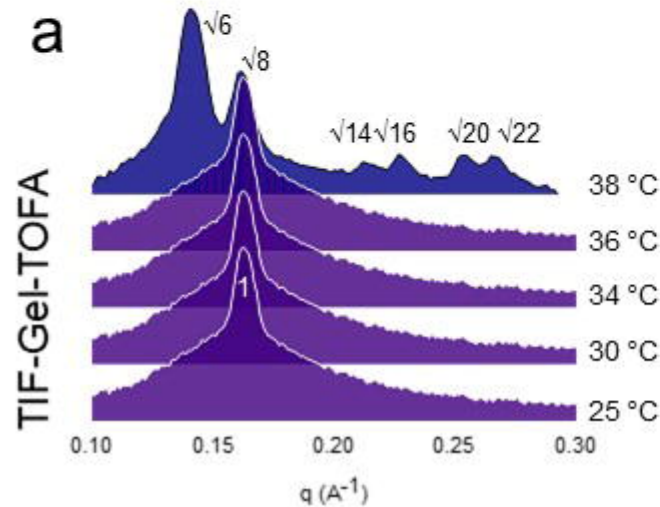
67. B. Chassaing, J. D. Aitken, M. Malleshappa, M. Vijay-Kumar, Dextran sulfate sodium (DSS)-induced colitis in mice, *Curr. Protoc. Immunol.* **104**, 15.25.1-15.25.14 (2014).
68. T. Fukuyama, S. Ehling, J. Wilzopolski, W. Bäumer, Comparison of topical tofacitinib and 0.1% hypochlorous acid in a murine atopic dermatitis model, *BMC Pharmacol. Toxicol.* **19**, 1–8 (2018).
69. L. F. Mager, V. H. Koelzer, R. Stuber, L. Thoo, I. Keller, I. Koeck, M. Langenegger, C. Simillion, S. P. Pfister, M. Faderl, V. Genitsch, I. Tcymbarevich, P. Juillerat, X. Li, Y. Xia, E. Karamitopoulou, R. Lyck, I. Zlobec, S. Hapfelmeier, R. Bruggmann, K. D. McCoy, A. J. Macpherson, C. Müller, B. Beutler, P. Krebs, The ESRP1-GPR137 axis contributes to intestinal pathogenesis, *Elife* **6** (2017), doi:10.7554/eLife.28366.
70. C. Moolenbeek, E. J. Ruitenber, The “Swiss roll”: A simple technique for histological studies of the rodent intestine, *Lab. Anim.* **15**, 57–59 (1981).
71. U. Erben, C. Loddenkemper, K. Doerfel, S. Spieckermann, D. Haller, M. M. Heimesaat, M. Zeitz, B. Siegmund, A. A. Kuhl, A guide to histomorphological evaluation of intestinal inflammation in mouse models, *Int. J. Clin. Exp. Pathol.* **7**, 4557–4576 (2014).
72. S. E. Liyanage, P. J. Gardner, J. Ribeiro, E. Cristante, R. D. Sampson, U. F. O. Luhmann, R. R. Ali, J. W. Bainbridge, Flow cytometric analysis of inflammatory and resident myeloid populations in mouse ocular inflammatory models *Exp. Eye Res.* **151**, 160–170 (2016).
73. M. R. Spalinger, M. Schwarzfischer, L. Hering, A. Shawki, A. Sayoc, A. Santos, C. Gottier, S. Lang, K. Bäbler, A. Geirnaert, C. Lacroix, G. E. Leventhal, X. Dai, D. Rawlings, A. A. Chan, G. Rogler, D. F. McCole, M. Scharl, Loss of PTPN22 abrogates the beneficial effect of cohousing-mediated fecal microbiota transfer in murine colitis, *Mucosal Immunol.* **12**, 1336–1347 (2019).

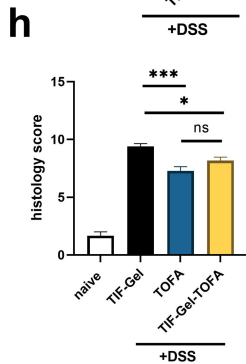
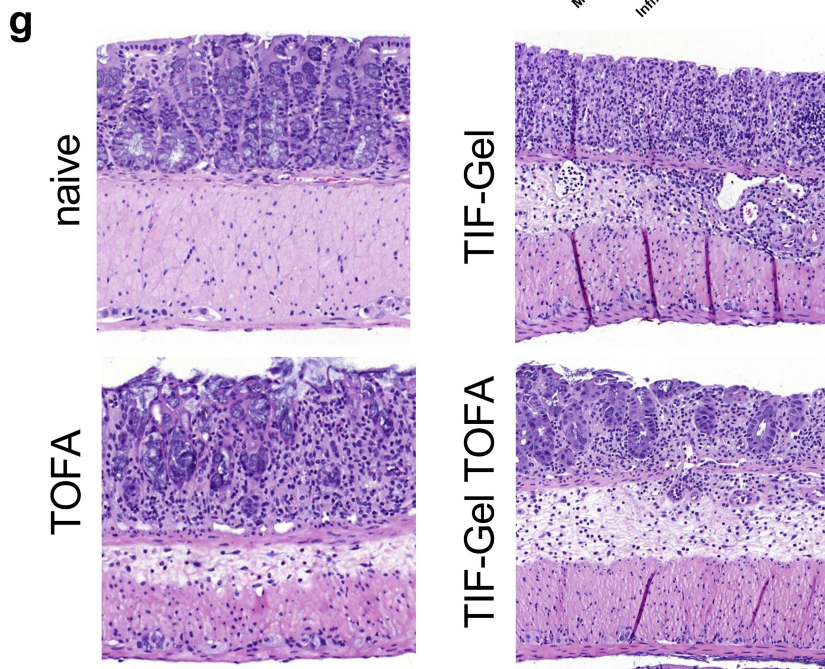
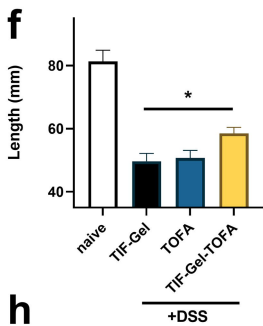
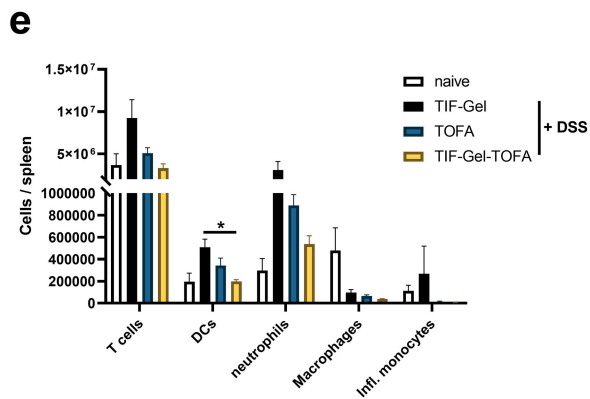
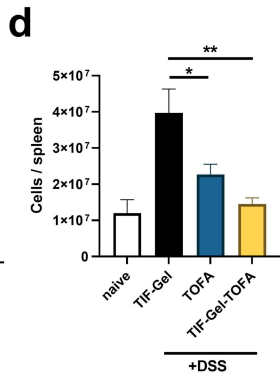
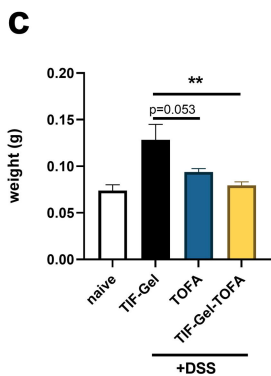
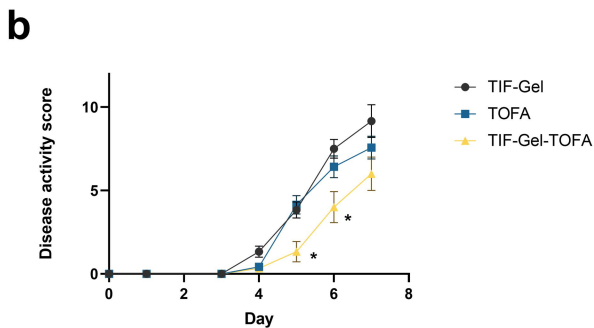
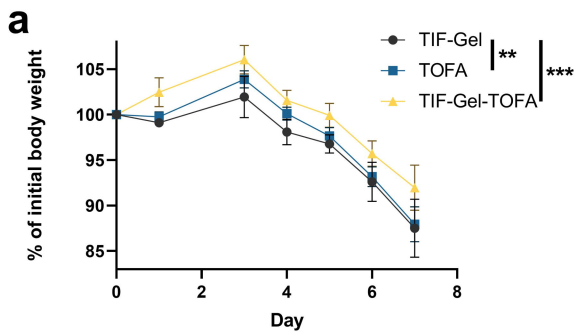




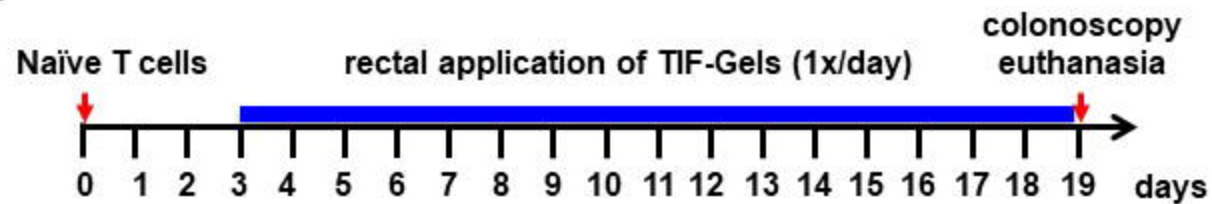
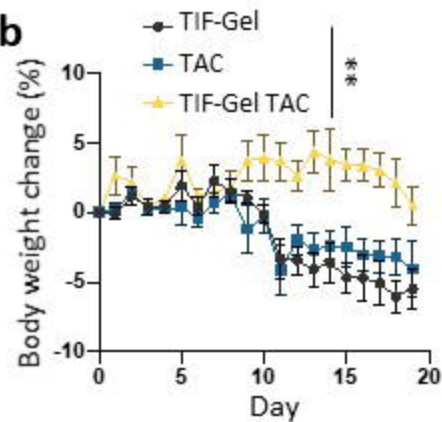
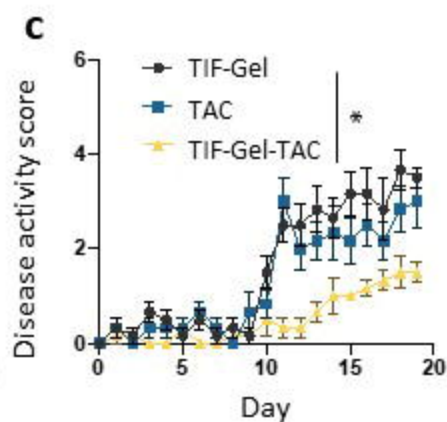
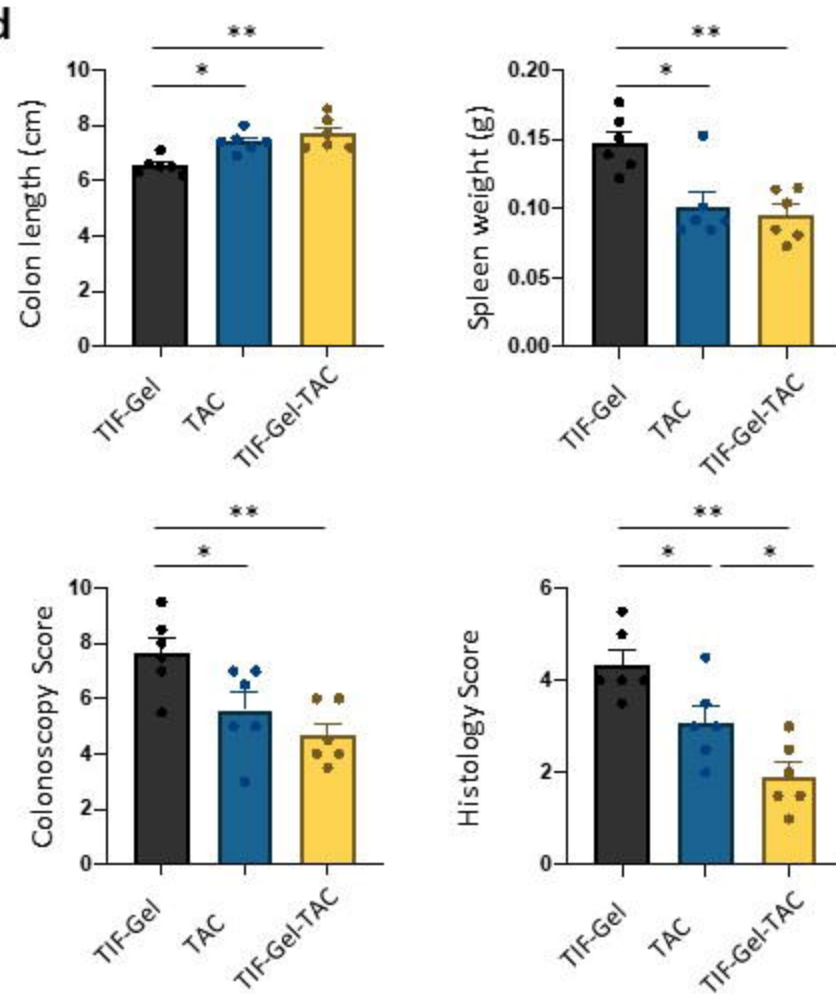
**a****b****c****d****e****f**

X-ray beam is directed at the TIF-Gel incubated at different temperature







**a****b****c****d****e**